SYNTHESIS AND CHARACTERIZATION OF GRAPHENE ENWRAPPED METAL OXIDE NANOCOMPOSITES FOR VISIBLE LIGHT-DRIVEN PHOTO-ELECTROCHEMICAL APPLICATION

BY

MOHAMMED ISAMELDEEN IBRAHEM ABDALWADOUD

A Thesis Presented to the
DEANSHIP OF GRADUATE STUDIES

KING FAHD UNIVERSITY OF PETROLEUM & MINERALS

DHAHRAN, SAUDI ARABIA

In Partial Fulfillment of the
Requirements for the Degree of

MASTER OF SCIENCE

In

CHEMISTRY

January 2017

KING FAHD UNIVERSITY OF PETROLEUM & MINERALS

DHAHRAN- 31261, SAUDI ARABIA

DEANSHIP OF GRADUATE STUDIES

This thesis, written by MOHAMMED ISAMELDEEN IBRAHEM ABDALWADOUD under the direction of his thesis advisor and approved by his thesis committee, has been presented and accepted by the Dean of Graduate Studies, in partial fulfillment of the requirements for the degree of MASTER OF CHEMISTRY.

Dr. SIDDIQUI, M.N.

(Advisor)

6/6/2017

Dr. AL-SAADI, ABDULAZIZ

Department Chairman

Dr. AL-ARFAJ, A.R.

(Member)

Dr. Salam A. Zummo
Dean of Graduate Studies

Dr. Mohammed Qamar
(Member)

7/6/17

Date

عمادة الدراسات العليا
DEANSHIP OF GRADUATE STUDIES

Dedication

This thesis work is dedicated to my parents, friends and Sudanese community at KFUPM.

ACKNOWLEDGMENTS

I would like to thank my creator Almighty ALLAH for giving me the patience, power and strength to finish this work, I also would like to express my sincere gratitude to everyone who helped me during my Study starting from KFUPM represented in Chemistry department for giving me this opportunity.

I would like to extend my sincere gratitude to my advisor Dr Mohammed Nahid Siddiqui for his patience, guidance and advice.

Beside my advisor, I would like to thank my thesis committee members Dr AL-ARFAJ and Dr Qamar.

I wish to extend my gratitude to the chairman of the chemistry department Dr Abdulaziz Alsaadi and the graduate coordinator Dr Bassam El-Ali for their time and countless help.

I would like to acknowledge the Center of Nanotechnology for their help during my research.

Finally, I would like to thank my Sudanese colleagues at chemistry department for their help and support.

TABLE OF CONTENTS

LIST OF FIGURES

LIST OF ABBREVIATIONS

GO: Graphene Oxide.

RGO: Reduced Graphene Oxide.

PEC: Photoelectrochemical.

XRD: X-Ray Diffraction.

SEM: Scanning Electron Microscope.

FE-SEM: Field Emission Scanning Electron Microscope.

TEM: Transmission Electron Microscope.

HR-TEM: High-Resolution Transmission Electron Microscope.

DRS: Diffuse Reflectance Spectroscopy.

BA: Benzyl alcohol.

TTIB: Titanium Tetraisopropoxide.

ABSTRACT

Full Name : Mohammed Isameldeen Ibrahem Abdalwadoud.

Thesis Title : Synthesis and Characterization of Graphene-enwrapped Metal Oxide Nanocomposites for Visible-light-driven Photo-electrochemical Application.

Major Field : Chemistry.

Date of Degree : January 2017.

Nanocomposites consisting of graphene and metal oxides (TiO_2 and WO_3) have been synthesized following a non-aqueous one-step solvothermal chemical method which is "benzyl alcohol route". Attempt have been made to extend the absorption edge of these nanostructures from ultraviolet to visible region. The synthesized nanocatalysts characterized by standard techniques such as TEM, FESEM, XRD, XPS, Diffuse reflectance spectroscopy, and so on. Photoelectrochemical behavior of the synthesized nanocomposite investigated under visible light (>420 nm) irradiation. The dependency of photocurrents on crucial factors such as the percentage of graphene, reaction time and reaction temperatures etc. have been investigated.

ملخص الرسالة

الإسم الكامل: محمد عصام الدين إبراهيم عبد الودود

عنوان الرسالة: توليف وتوصيف أكاسيد المعادن المغلفة بالجرافين وإستخدامها فى التطبيقات الإلكتروضوئية

التخصص: الكيمياء

تاريخ الدرجة العلمية: يناير 2017

المركبات النانوية المؤلفة من الجرافين و أكاسيد المعادن (ثانى أكسيد التيتانيوم و ثالث أكسيد التنجستون) تم تحضيرها فى وسط غير مائى بإتباع طريقة التذويب الحرارى الكيميائية بخطوة واحدة, والتى يطلق عليها "جزر الكحول البنزيلى".

أجريت العديد من المحاولات لجعل هذه المركبات تمتص الضوء المرئي بالإضافة للضوء فوق البنفسجى الذى تمتصه بطبيعتها.

هذه المركبات تم توصيفها بإتباع عدد من التقنيات مثل أشعة الحيود السينية, والمجهر الإلكترونى الإنتقالى, ومجهر المسح الإلكترونى...الخ.

.السلوك الإلكتروكيميائى لهذه المركبات تمت دراسته بتعريضها للأشعة المرئية

إعتمادية التيار الضوئى الناتج على بعض العوامل مثل النسبة المئوية للجرافين, زمن التفاعل و درجة حرارة التفاعل...الخ تمت دراستها وتم تحديد الظروف المثلى للحصول على أعلى تيار.

CHAPTER 1

INTRODUCTION

1.1 Background:

Between the optimists who believe that the oil production rate will rise to peak in 2100 at nearly 105 million barrels per day (Mbpd), and decline to 40 Mbpd by 2400, and the pessimists who their trust in the oil era is over, and their reports speak that the peak oil occurred in 2009 at a production rate of 86 Mbpd and world oil production will decline to 40 Mbpd by 2050, there are no doubt, that oil peaking become an academic debate with no concurrence to date, but it's worth mentioning that the majority of scientists argues that the global oil production has either peaked already or will be peaking soon[1]. A human being is directly and inseparably associate to energy, from history point of view the energy consumption started with food, but when the societies developed upon the industrial era they began to use the stored chemical energy in fossil fuels and convert it into work, heat and Carbon Dioxide[2]. The strong dependence on fossil fuels as an energy source made our economy highly sensitive to price spikes (in 2015 crude oil prices around 60$ a barrel while it was less than 3$ when the Fujishima's paper get published on 1972) [2], on the other hand, the excessive use of fossil fuels raises a serious environmental crisis like air pollution and global warming.

Thus looking for renewable, clean alternative to fossil fuels is a matter of utmost urgency, one of the most attractive possibilities which grab the attention of scientific community is the conversion of solar energy into Hydrogen energy (which is widely considered to be the

fuel of the future) and/or electricity by splitting water using photoelectrochemical (PEC) cell[3],[4],[5], because the energy content of 1.5 hours from sunlight is equivalent to that consumed by the whole world's population[6]. Since that time photocatalytic water cleavage received much attention from scientific and industrial communities. The term "photocatalytic reaction'' can be defined as a chemical reaction induced by photo-absorption of a solid material, known as a ''photocatalyst,'' which remains unchanged during the reaction[7]. Water splitting by visible light have been considered as a highly prized goal of photoelectrochemical research, and the obtained efficiency for the conversion of solar light energy into chemical energy are about 7%, it is reported that the efficiency reached 20% but using materials with too much cost which cannot be used for large-scale production[8],[9],[10]. Thus, developing materials which can produce high current with low overpotential (overpotential is the additional voltage required to drive a reaction at the desired rate or current density) using the simple approach with low cost was attracted the attention of the researchers working in the field of energy.

Kingdom of Saudi Arabia is located in the so-called "sun belt" with widespread desert land and year-round clear skies with average amount of sunlight falling on Saudi Arabia about (2200 thermal kWh/m^2,kWh= kilowatt hours), Thus it can take advantage of solar energy[11], and this huge amount of energy can be utilized to produce Hydrogen by water splitting. The Solar Hydrogen Production Plant situated at the Solar Village, Riyadh produced 463 m^3 of hydrogen per day at normal pressure[12].

There are several approaches for solar hydrogen production, such as:

(1) Electrolysis of water using a solar cell.

(2) Reforming of Biomass.

(3) Photocatalytic or photoelectrochemical water splitting[13].

Our interest lies in the last method; Because of its simplicity and the powdered photocatalyst can be used large scale applications, enormous research has been done to find an efficient semiconductor photoelectrodes, but still its challenging reaction even if the research history is long.

Titanium dioxide (TiO_2) and Tungsten oxide (WO_3) consisting of d^0 metal cations (Ti^{4+} and W^{6+}) with a wide band gap, which can cover the potential of water reduction and oxidation, appears to be excellent photocatalysts for photoelectrochemical applications. But since the main limitation in the photocatalytic activity reaction is electron-hole recombination process, different kinds of materials used to trap the electrons so it can slow the recombination rate, among this materials graphene emerged as one of the most promising materials due to its characteristic specifications. Several methods have been used to synthesize hybrid organic-inorganic nanocomposites, one of the most suitable, surfactant-free, simple and one-step approaches is “benzyl alcohol route” by mixing the metal oxide precursor with benzyl alcohol in Teflon hydrothermal vessel autoclave and heat it at different temperatures and times.

1.2 Research Methodology:

"Benzyl alcohol route" has proven to be a powerful method for the synthesis of oxide nanoparticle, offering merits such as high crystallinity, high reproducibility and the ability to control the crystal growth of the synthesized oxides without use of additional ligands [14], Pengyu *et al* used Titanium isopropoxide as a Titanium precursor, and mixed it with the dispersion of reduced graphene oxide (RGO) in benzyl alcohol, with addition of acetic acid at 180 ^{0}C [15]. And since the boiling point of benzyl alcohol is 205.3 ^{0}C, we used single-step hydrothermal reaction at higher temperatures without any other chemicals, it is worth mentioning that benzyl alcohol act as a solvent and as a reducing agent at the same time. And RGO synthesized using modified Hummers method [16].

Approximately 2 *mmol* of metal precursor dissolved in 20 ml benzyl alcohol with vigorous steering until we get a clear solution, followed by the addition of graphene oxide (GO) solution. Then, the resulting solution will be transferred to a 45 ml Teflon hydrothermal vessel autoclave and heated it for different temperatures and times. At the end of the reaction, obtained product will be washed using acetone and ethanol followed by centrifugation every time for 12000 RPM. Finally, the washed product will be dried and collected. Then we will prepare the thin films by using 10 mg from the catalyst add it to a solvent mixture (8 ml deionized water, 2 ml isopropanol, and 40 µL Nafion 5%wt), followed by sonication for 15 - 20 minutes until we get a homogeneous solution. Then we will take 1 ml of this solution (contain 1 mg catalyst) and deposit it on 1 cm^2 of a glass substrate coated with Indium Tin Oxide (ITO) at 60 ^{0}C.

1.3 Research Objectives:

The objectives of this research are divided into four parts:

1- To develop synthesis method to produce visible-light-active graphene/TiO_2 nanocomposite in a single step.

2- To develop synthesis method to produce visible-light-active graphene/WO_3 nanocomposite in a single step.

3- To characterize these nanocomposites by advanced instrumental techniques.

4- To investigate the photoelectrochemical behavior under visible light.

1.4 Instrumentation:

Samples were characterized using several techniques, such as:

- X-Ray Diffraction (XRD).
- Field Emission Scanning Electron Spectroscopy (FE-SEM).
- Transmission Electron Microscopy (TEM).
- X-Ray Photoelectron Spectroscopy (XPS).
- UV-Vis Diffuse Reflectance Spectroscopy (DRS).
- Electron Paramagnetic Resonance (EPR).

To study the photoelectrochemical activity we used three electrodes set up photoelectrochemical cell directly connected to a potentiostat, Saturated Calomel Electrode (SCE) as a reference, Platinum electrode as a counter electrode and working electrode (ITO-Coated glass plate).

CHAPTER 2

LITERATURE REVIEW

It clearly appears that the idea of converting light into electric power or chemical fuel was firstly discovered by the French scientist Edmond Becquerel on 1839, he Studied the (AgCl /electrolyte/metal) system, and he observed that a current generated between the AgCl and the metal electrodes when AgCl was exposed to light, including sunlight, which termed as *Becquerel effect* [9][17].

Photoelectrochemical water splitting process is based on the conversion of light energy into electricity inside a cell consists of two electrodes dipped in an aqueous electrolyte, in which one of those electrodes made of a semiconductor exposed to light and have the ability to absorb it, followed by utilizing the electricity for water electrolysis [17]. Light can provide energy to the reaction with the assistant of applied chemical or electrical bias mainly for two reasons which are the insufficient PEC cell voltage and overcome slow kinetics [4].

2.1 Bases of photocatalytic water splitting:

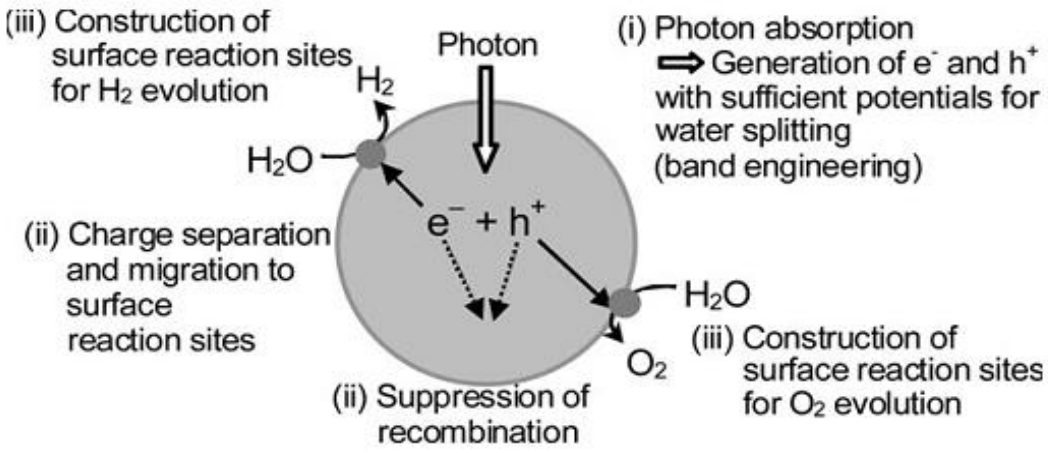

Figure 1 Showing the main process in photocatalytic water splitting

Firstly (i) the absorption of photons results in intrinsic ionization of the semiconductor which leads to the generation of charges (electron-hole pair) which causes redox reaction.

$$2hv \longrightarrow 2e^- + 2\,h\cdot \qquad (1)$$

Where *h* is Planck's constant, *v* the frequency, (e^-) the electron and ($h\cdot$) is the electron hole. If the energy of the photons (*hv*) is equal to or larger than the band gap, then reaction (1) may take place.

The second step (ii) is the separation of these charges and suppress the recombination process, it is worth mentioning here that the smaller the particle size photocatalyst, the shorter the distance for generated charges to reach to reaction sites on the surface which decrease the recombination probability.

The final step (iii) is the water splitting on the surface of the catalyst if there are no active sites on surface electrons and holes will recombine and no redox reaction will take place, to solve this problem generally Co-Catalyst used to introduce active sites. For the final step although both crystallinity and surface area are important, specifically for water splitting high degree of crystallinity is often needed rather than high surface area because the recombination between the photo-generated charges is a real problem for uphill reactions [13].

The holes generated at the valance band interact with water molecules and at the photo-anode/electrolyte interface the following reaction takes place:

$$2h\cdot + H_2O_{(liquid)} \longrightarrow 1/2\ O_{2\ (gas)} + 2H^+ \qquad (2)$$

While the electrons generated at the conduction band transfer to the cathode through the external circuit resulting in the formation of Hydrogen by the reduction of Hydrogen ion formed in reaction (2) as follow:

$$2H^+ + 2e^- \longrightarrow H_{2\ (gas)} \qquad (3)$$

The main difference between the photocatalytic water splitting and photoelectrochemical water splitting are the location of the sites for Reaction (2) and (3). In the photoelectrochemical cell, these reactions take place at the photo-anode and cathode respectively. While in the photo-catalytic process both reactions take place on the surface of the photocatalyst, which exhibits the functions of both anode and cathode. Practically that means in the photoelectrochemical cell Hydrogen and Oxygen will come out separately, while in the photocatalytic cell a mixture of both gasses is evolved [17].

Collecting and storing solar energy into chemical bonds of a nanostructured transition metal oxide inspired too many researchers and gained their interest increasingly, especially n-type metal oxides such as TiO_2 and WO_3 which studied intensively due to their high chemical stability, low costs and environment friendliness.

2.2 Benzyl Alcohol Route:

To synthesize a crystalline metal oxides in a nanoscale a lot of methods have been reported in the literature, for instance, *Sol-Gel* approach which suffers from some drawbacks such as the precipitation of amorphous compounds in addition to the higher reactivity of metal precursor in water which make the control of metal oxide growth very difficult process[18]. For these reasons and others non-aqueous synthesis methods become more valuable than aqueous approaches, and since some of the surfactants are toxic and have a side reaction a huge number of scientists focusing on using solvent can behave as a reactant as well as controller agent for the particle growth.

When the donor of Oxygen is not water then the Sol-gel approach considered as a non-hydrolytic, for instance, "*alkoxide route*" and "*ether route".* In "*alcohol route*" the reaction depends on the nature of alcohol whether it's primary, secondary or tertiary. Although the "*alcohol route*" has been much less explored compared to alkoxide route and ether route yet "*benzyl alcohol route"* proven to be successful for the synthesis of highly crystalline metal oxides[19]. Different roles can be played by the organic solvent such as Oxygen provider for the metal oxide, crystal growth controller, particle shape influencer and sometimes assembly behavior determiner[20].

2.3 Titanium Dioxide based material for water splitting:

The research on photo-assisted electrochemical water oxidation was initiated more than four decades ago just before 1973 oil crisis by the pioneer work of Fujishima and Honda, when photoelectrochemical water splitting into H_2 and O_2 was realized on an N-type Titanium Dioxide single-crystal electrode to drive the oxidation of water by band gap excitation and evolving Hydrogen gas at a Platinum secondary electrode [21]. Since that time TiO_2 has widely studied due to it is abundance, high stability, low cost, high corrosion resistance, nontoxicity and most efficient and environmentally benign photo-catalyst, Nevertheless Titania has some drawbacks such as wide band gap (3.2 eV) which is lowering the absorption ability of solar light, higher recombination rate of photogenerated electron-hole pairs (10^{-9} s), low quantum yield and difficulty on recovery from treated water [15][22]. Thus, much research has been focused on enhancing the photocatalytic activity by shifting the absorption edges toward the visible light and increase the lifetime of charge separation.

To split water sufficiently by solar light, the band gap of the semiconductor anode must be larger than 1.23 eV, which is the theoretical value of the water electrolysis [23], To say that a semiconductor photocatalyst is good, having a suitable band gap is not enough (band gap is the smallest energy difference between the top of the valence band and the bottom of the conduction band), but also the Conduction Band energy edge should be more negative than the potential needed to evolve Hydrogen, and the Valence Band energy edge should be more positive than the potential needed to evolve Oxygen [24].

TiO_2 exist mainly in three different allotropic forms with different crystal shapes: anatase (tetragonal), rutile (tetragonal) and brookite (orthorhombic) all of them represent distorted octahedral as illustrated in Figure 2.

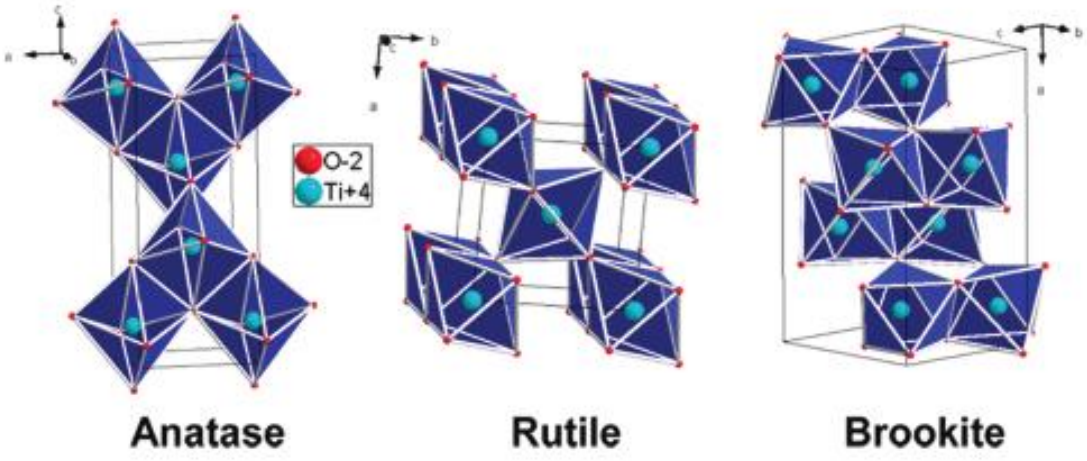

Figure 2 Crystalline forms of Titania.

Although the anatase structure consists of edge-sharing TiO_6 octahedra, the rutile and the brookite structures exhibit both corner- and edge- sharing configurations[25].

Titania have a low solar photoconversion efficiency because of the wide band gap, whether it is anatase (3.2 eV) or rutile (3.0 eV) so when it is exposed to sunlight it can only excited under irradiation of UV light which represent about 4% from the incoming solar energy to the Earth surface [26], engineering the photocatalyst band gap to be less than 3.0 eV was a target for a huge number of researchers in this area, one of the more promising techniques to achieve visible light activity is by nonmetal element doping such as Nitrogen and Sulfur [27], and carbonaceous material [28].

Since the mid-1990s research on the area of carbonaceous nanomaterials, such as carbon black, graphite, carbon nanotubes, fullerenes, graphene and more have increased dramatically, because of their unique properties, and it is a beneficial effect on the photocatalytic activity of TiO_2 have been reported [28]. Among these carbonaceous graphene received and still receiving much more attention since it is discovery by the group led by Andre Geim in 2004 [29], and was the last allotrope to be discovered using "Scotch tape technique" with one Carbon sp^2 atom thick honeycomb lattice, and one of the strongest materials ever, for that graphene has been considered by many as a revolutionary material with remarkable properties, such as considerable surface area (2630 m^2g^{-1}), huge electron mobility (~200,000 cm^2Vs^{-1}), very high thermal conductivity (more than 3000 W mK^{-1}), good optical transparency (97.7%), electrical conductivity of (4.84 – 5.30) 103 W mK^{-1}, and good chemical stability, for all of these and many other reasons research on graphene field is one of the fastest growing areas of science and surrounded by a lot of hype but also with hope [30],[31]. In photocatalysis, specifically electrical and optical properties are the most convenient.

According to the literature, composites of TiO_2, WO_3 or other metal oxides with graphene based-nanosheets can be synthesized by different approaches: The simplest way to prepare graphene oxide (GO)-TiO_2 composite is by using sonication method which consists of two steps, mixing and sonication, firstly used by Williams *et al*, but it's generally suffering from weak interaction between the two phases [32]. Secondly the sol-gel process which is the widely explored approach to producing GO-TiO_2 composites, in this method GO which have the ability to form Hydrogen bonding due to the presence of hydroxyl surface groups

and also can make hydroxo- or oxo-bridges with metal centers, Titanium alkoxide precursors generally used [33], and there are some modification for this method [34].

Thirdly the hydrothermal and solvothermal methods, this approach usually performed in stainless steel autoclaves under the control of temperature and/or pressure, at the end of the reaction partial reduction of GO commonly happen resulting in reduced graphene oxide RGO, in some cases if reduced agent used graphene sheets can be obtained [32], [28]. To reduce GO to RGO environmentally friendly reduced agent have been used such as glucose replacing hydrazine [33]. The last method is doping or metal deposition, generally used to improve the efficiency of the materials, for instance, Neppolian *et al* deposited Pt on GO-TiO_2 composites [34].

2.4 Tungsten Oxide based material for water splitting:

Tungsten has a rich history since the earlier discovery by Woulfe, and the elemental symbol "W" coming from the word wolfram which was the original name of Tungsten, few years after and in 1841 the chemist Oxland granted a patent on the procedure he invented to prepare Tungsten trioxide[35]. WO_3 firstly used on photocatalytic reaction in 1976 by Hodes, Cahen and Manassen when they demonstrated for the first time the possibility of splitting water by WO_3 photoanode, and they used Platinized Platinum oxygen counter electrode, SCE as aa reference electrode immersed in 1 N H_2SO_4 in a quartz cell under illumination of ~ 100 mW cm^{-2}[36]. and since that time considered to be one of the most popular Oxides that extensively studied and believed to be alternative for Titania for water splitting under visible light irradiation, and that for several reasons for instance the band gap is 2.8 eV so mainly absorbs in the near ultraviolet and blue regions of the solar

spectrum up to 500 nm, which can capture nearly 12% of the solar spectrum (while in case of TiO_2 approximately 4%), compared to TiO_2 band gap (3.0-3.2 eV, in addition, WO_3 has moderate hole diffusion, good electron transport properties, highly resistant to photo-corrosion with good chemical stability in acidic solutions[37],[38],[39]. Using TiO_2 and WO_3 as a photoanode theoretically the maximum conversion efficiency of solar energy into Hydrogen is 4.8% in WO_3 case, while 2.2% for TiO_2 in a photoelectrochemical water splitting device[40].

Moreover, WO_3 is recognized as one of the few n-type semiconductors. Although the valence band edge of WO_3 is sufficiently positive to oxidize water, the conduction band is not negative enough to reduce water and produce Hydrogen, furthermore to make WO_3 absorb light significantly we should make a thick film according to its indirect band gap. Thick film electrode usually increases the electron-hole recombination rate and decrease the photocatalytic activity consequently[39]. Generally, Tungsten Oxide has poor charge mobility thus it produces a very low photocurrent. Practically, one of the biggest obstacle hindering the development of WO_3 as a photocatalyst is the high rate of electron-hole recombination process because of slow oxidation reaction combined with poor charge mobility at the electrode/electrolyte interface. To enhance WO_3 solar absorption ability and decrease the recombination rate of photogenerated electron-hole, scientists utilized co-catalysts loading, doping, Z-scheme photocatalysis, crystal facet tuning, heterojunction construction, nano-architecture design and dye sensitization etc. among this graphene attracted considerable interest and was thought to be one of the most promising candidates due to its ability to enhance the mobility of charge carriers (20 000 $cm^2\ V^{-1}\ s^{-1}$ at room temperature) and its high specific surface area (2630 $m^2\ g^{-1}$) so it's possible that Graphene

might suppress the charge recombination[41][42]. WO_3-Graphene composites used for several applications such as sensors, photo-degradation, oxygen evolution using a suspension reaction system and PEC studies.

CHAPTER 3

RESULTS AND DISCUSSION

3.1 TiO_2/RGO nanocomposite Synthesis and photocatalytic activity:

3.1.1 Titanium Dioxide synthesis:

2.7 *mmol* from Titanium Tetra Iso Propoxide (TTIP) which typically equal 0.8 ml, mixed with 20 ml from Benzyl Alcohol (BA) with vigorous steering until we get a clear yellow solution, Then, the resulting solution transferred to a 45 ml Teflon hydrothermal vessel autoclave and heat it for different temperatures (210 ^{0}C, 220 ^{0}C, 235 ^{0}C and 250 ^{0}C) and times (12h, 24h, 36h, and 48h) for optimization. At the end of the reaction, the obtained product washed five times using acetone (40 ml, three times) and ethanol (25 ml, two times) followed by centrifugation every time for 12000 RPM. Finally, the washed product dried overnight and collected.

3.1.2 Reduced Graphene Oxide Synthesis:

150 ml from Sulfuric acid was placed inside 250 ml flask and put it inside ice path and 2.0 gram of graphite was added slowly. After that 15.0 gram of Potassium dichromate added slowly for 30 min. Followed by addition of 10 ml distilled water drop by drop, after that the reaction flask was closed using parafilm and left stirring for one week.

After one week, the solution placed in a beaker with stirring, 1200 ml distilled water added and the whole solution centrifuged, the resulting precipitate washed ten times with water and the product dried overnight inside the oven at 110 ^{0}C.

3.1.3 Titanium Dioxide/Reduced graphene oxide synthesis:

Calculated amount from Reduced Graphene Oxide (RGO) dissolved in (BA) by powerful sonication using probe sonication for three hours, taking exact millimeters from this solution depend on the percentage of RGO needed in the nanocomposite (0.5%, 1.0%, 2.5%, 5.0% and 10.0%), then mixed with 2.7 mmol from Titanium Tetra Iso Propoxide (TTIP) which typically equal 0.8 ml, mixed with (20 ml – the milliliters from BA used with RGO) from Benzyl Alcohol (BA) with vigorous steering until we get a clear yellow solution, Then, the resulting solution transferred into a 45 ml Teflon hydrothermal vessel autoclave and heat it for different temperatures (210 ^{0}C, 220 ^{0}C, 235 ^{0}C and 250 ^{0}C) and times (12h, 24h, 36h and 48h) for optimization. At the end of the reaction, the obtained product washed five times using acetone (40 ml, three times) and ethanol (25 ml, two times) followed by centrifugation every time for 12000 RPM. Finally, the washed product dried overnight and collected.

3.1.4 X-Ray Diffraction (XRD):

The crystalline Titanium dioxide was characterized by powder X-Ray Diffractometer rigaku rint-2500. Radiation Cu Ka lamb: 1.54060, λ=1.54056 A, 2Ɵ degree range was between 20 – 80 and the scan rate was 2.

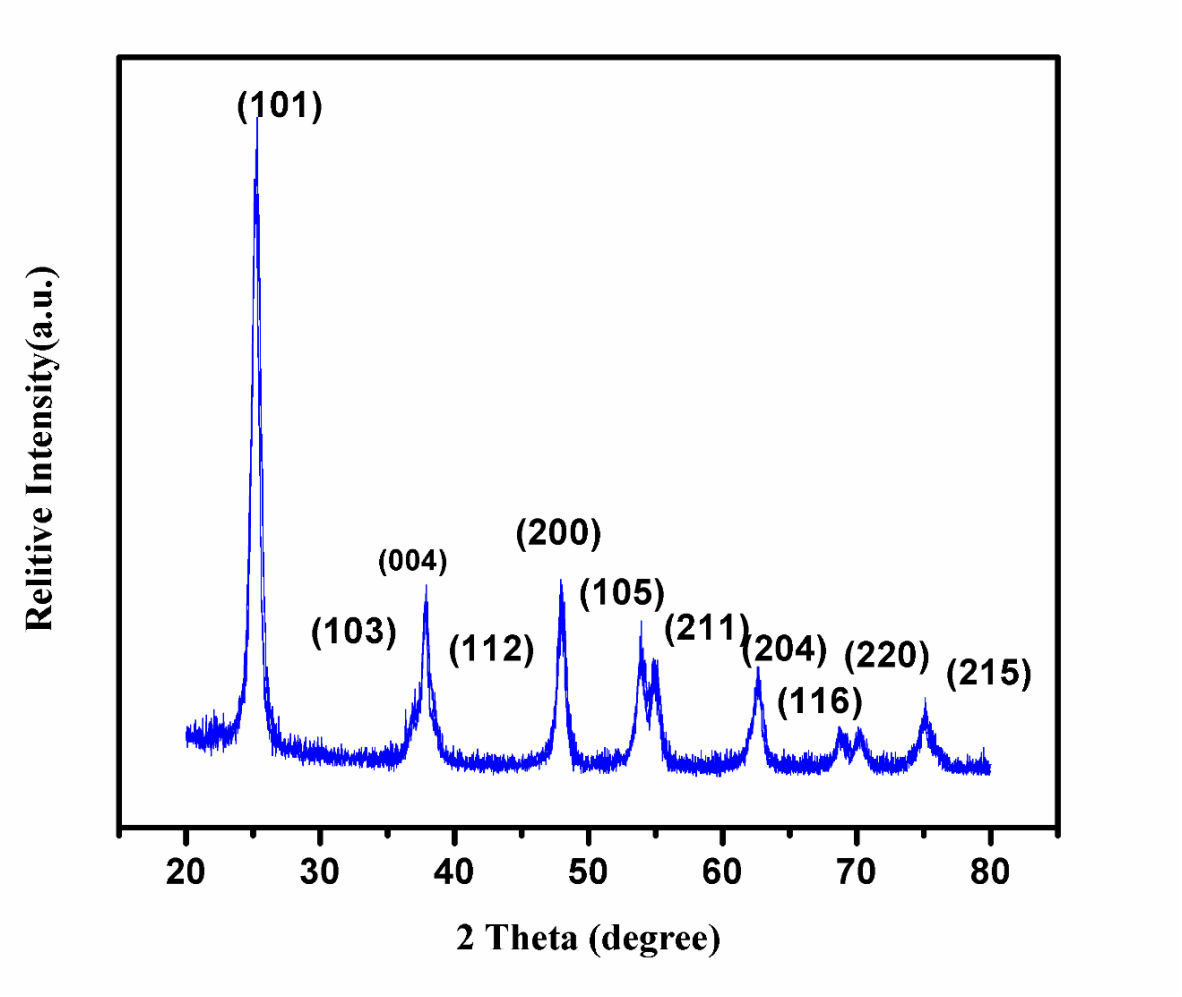

Figure 3 XRD of pure TiO_2 obtained at 250 ^0C

Mixing Titanium tetra isopropoxide with benzyl alcohol under the condition mentioned end up with tetragonal Titanium Dioxide (Anatase) as XRD peaks in Figure 3 showing with lattice constants *a=3.777000 Å c=9.501000 Å* (ICDD 00-089-4921), the diffraction peaks can be indexed as (101), (103), (004), (112), (200), (105), (211), (204), (116), (220), (215) planes, respectively. And there is no evidence that other phases of TiO_2 are present. Figure 4 illustrating the XRD patterns of pure Titania at different temperatures. While Figure 5 showing a comparison between XRD patterns of pure Titania and nanocomposite of Titania with 5% RGO. for TiO_2/RGO 5% sample the presence of RGO can't be detected

due to weak and broad characteristic peak at 24.5 ^{0} which was covered by the strong (101) plane[43].

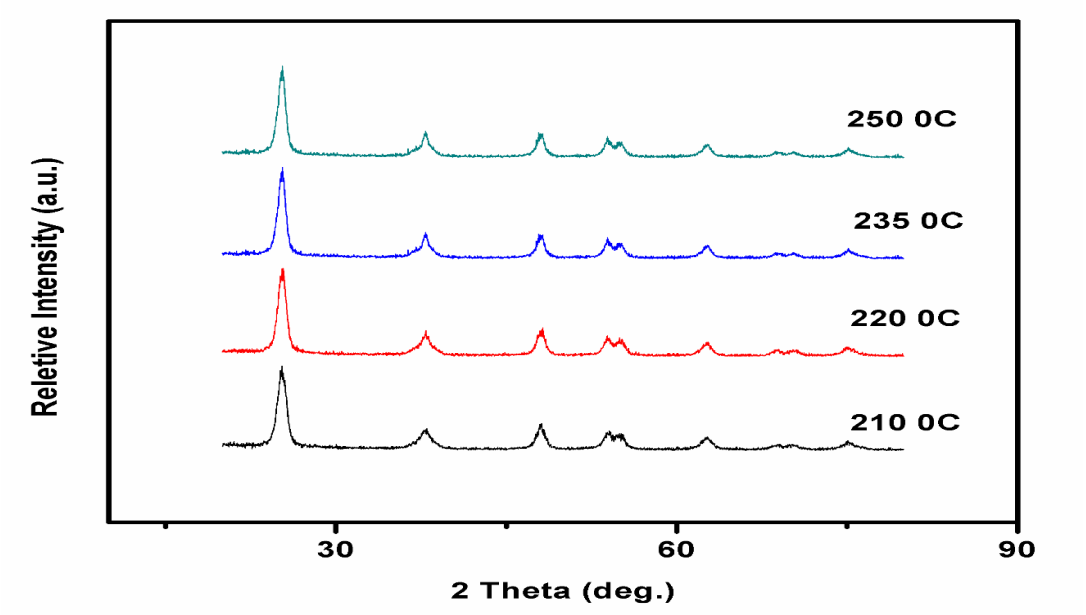

Figure 4 XRD of pure TiO_2 at different temperatures

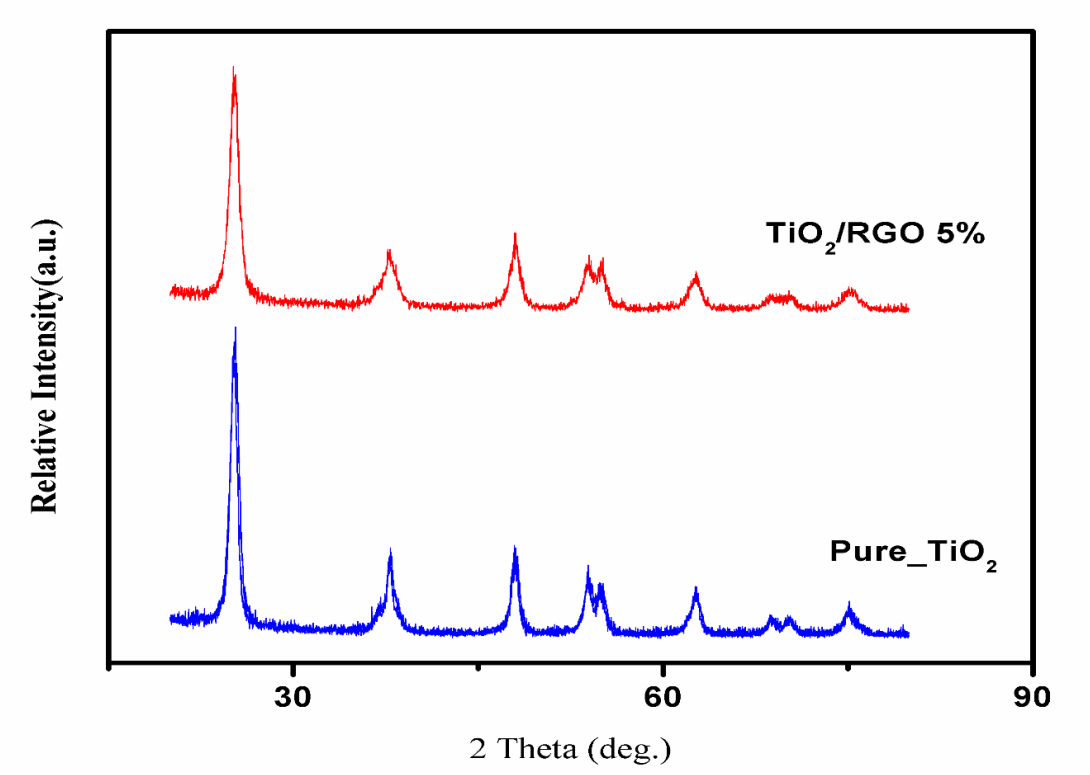

Figure 5 XRD patterns of TiO_2 and TiO_2/RGO 5%

Figure 4 illustrate X-Ray diffraction peaks of the as-synthesized TiO_2 in deferent reaction temperatures, and since the difference between these temperatures is so small, almost no change has been noticed on their diffraction peaks intensity meaning the crystallinity remained as it's.

3.1.5 Scanning Electron Microscope (SEM):

Scanning Electron Microscope was carried out with (FESEM, Tescan Lyra-3). SEM micrographs of pure titania and nanocomposite of Titania and RGO showed spherical small particles in a micro sized scale. Nanoparticles within 30 to 60 nanometers have been detected.

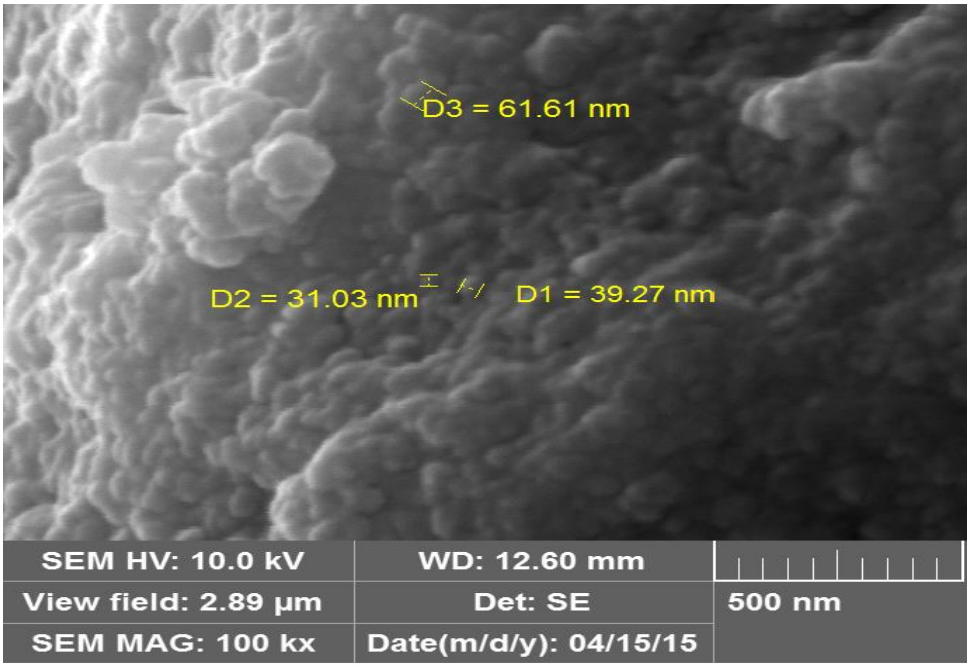

Figure 6 SEM of TiO_2

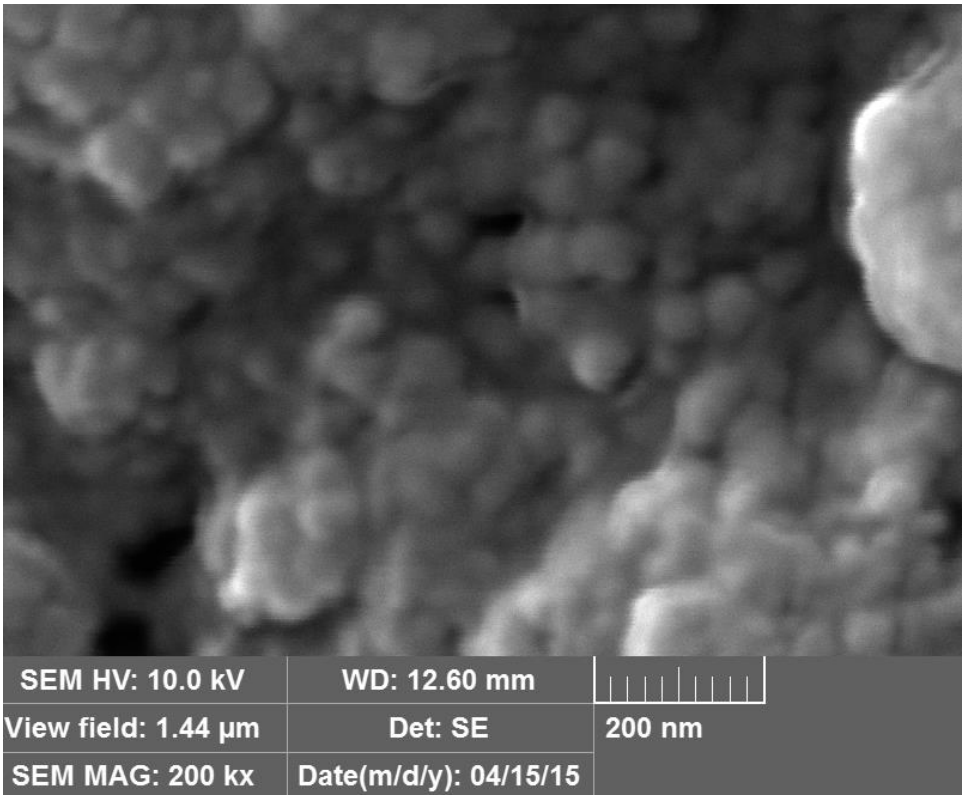

Figure 7 SEM of TiO_2/RGO 5%

3.1.6 UV-Vis Diffuse Reflectance Spectroscopy (DRS):

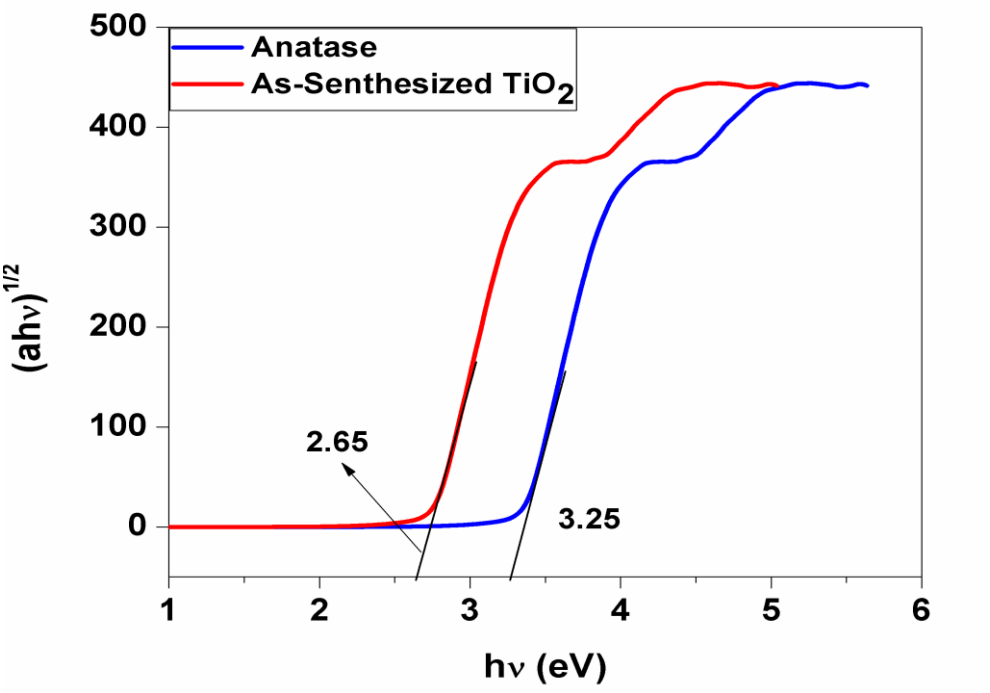

Figure 8 DRS of TiO_2_BA compared to commercial **TiO_2**

The optical response was analyzed by diffuse reflectance spectroscopy using (DRS, JASCO V-670). What we can learn from Figure 8 is the method we used which is benzyl alcohol route not only gave a highly crystalline TiO_2, but also helped on minimizing the band gap of TiO_2, so TiO_2 ability to absorb visible light is extended and the photocatalytic activity would increase as well. The band gap decreasing could be attributed to the formation of Ti^{3+} as a result of the reduction of Ti^{4+} by benzyl alcohol.

3.1.7 X-Ray Photoelectron Spectroscopy (XPS):

X-Ray photoelectron spectroscopy conducted using (XPS, Thermo Scientific ESCALAB 250Xi).

The change on chemical surface bonding can be detected by XPS technique. Figure 9 shows the XPS survey spectrum of the as-synthesized TiO_2 powder prepared by the reaction of TTIP with Benzyl alcohol at 250 ^{0}C for 24 hours. Peak positions were referenced internally to Carbon (C1s peak at 284.6 eV). XPS survey peaks show that the prepared TiO_2 contain only Titanium and Oxygen. The C element is attributed to the remaining carbon from the precursor solution and the adventitious hydrocarbon from the XPS instrument itself.

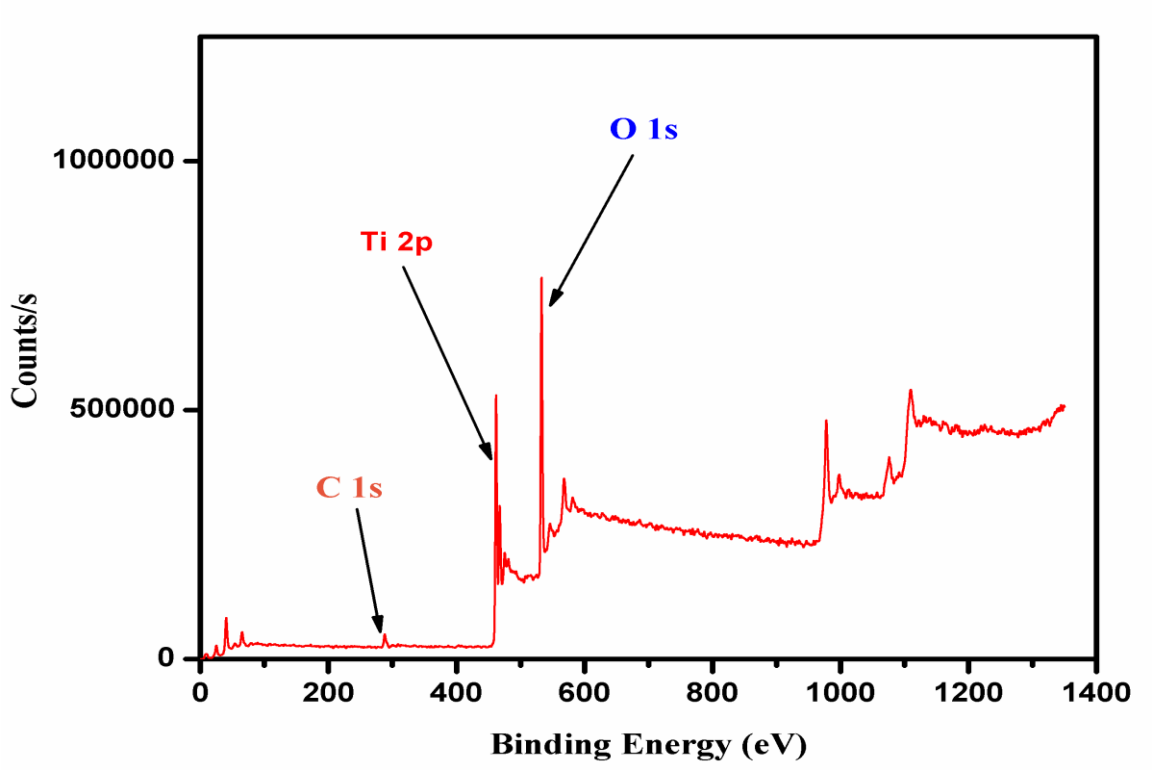

Figure 9 TiO2_BA Survey

The Ti 2p XPS shown in Figure 11 recorded to investigate the chemical states of Titanium, and to check the existence of Ti^{3+} (Oxygen vacancy). Titanium 2p peak are slightly shifted to lower energy which might confirm the partial reduction of Ti $^{4+}$ to Ti^{3+}, the same can be said for O 1s XPS in Figure 10. And this might suggest the formation of Oxygen vacancies,

and thus, the electrons pound to Titanium and Oxygen would migrate to this vacancy which work as electron trap. So XPS shift observed in Ti2p and O1s spectrum support the band gap result obtained by DRS in Figure 8.

Briefly the removal of one Oxygen atom from the lattice will leave 2 electrons, in case of Titania it's observed that Ti^{3+} entity is emerged as a result of filling the empty states of Ti ions by those 2 electrons, this process called Oxygen vacancy[44]. And since the Oxygen vacancy affect the migration, transfer and trapping of the photogenerated electrons and holes, then it's playing an important role on enhancing the photocatalytic activity.

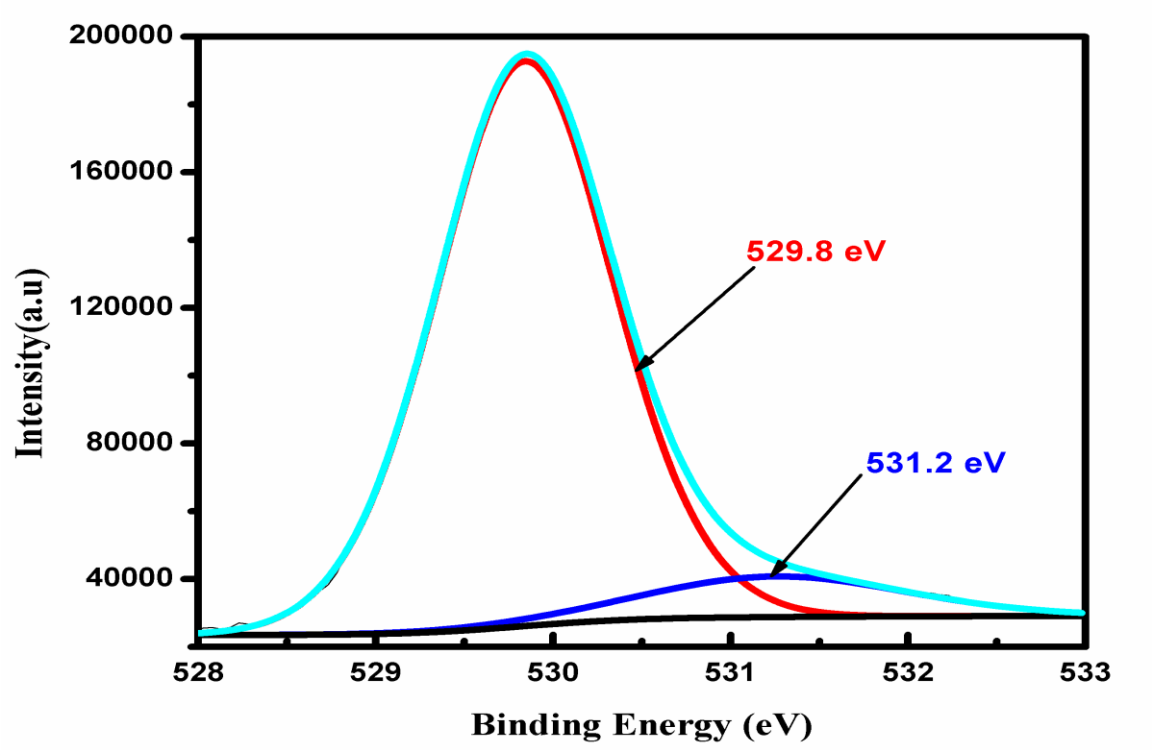

Figure 10 O 1s XPS

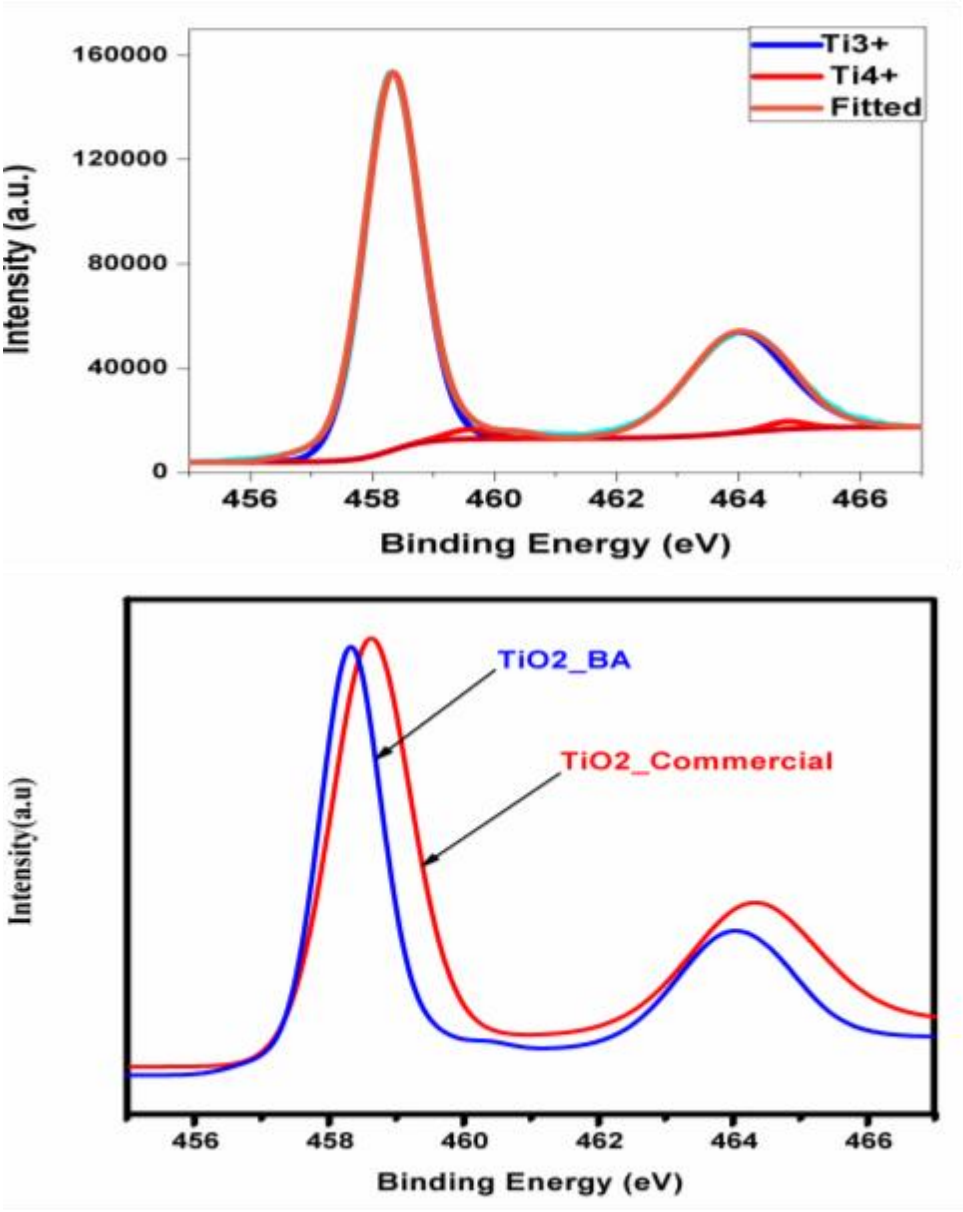

Figure 11 Ti 2p XPS

3.1.8 Electron paramagnetic resonance (EPR):

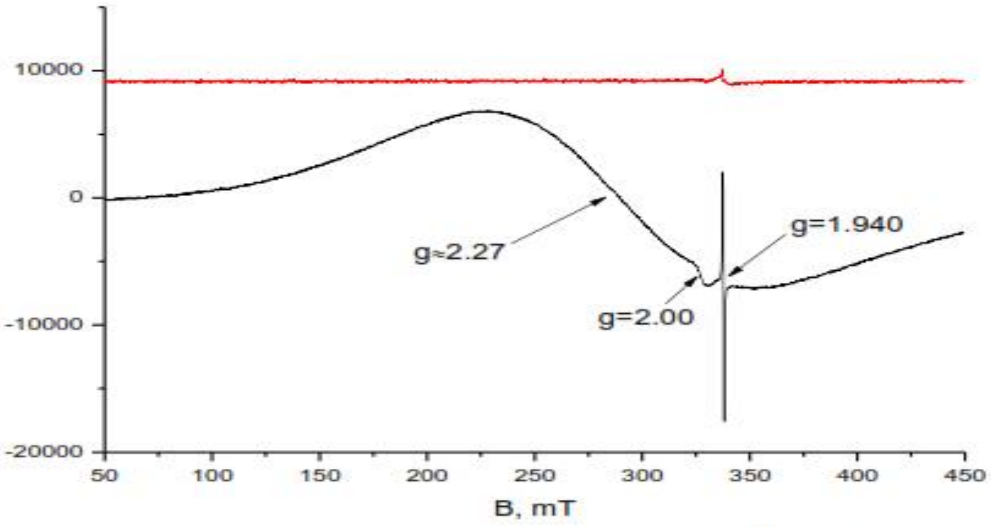

Survey EPR spectra of synthesized (black) and commercial (red) samples.

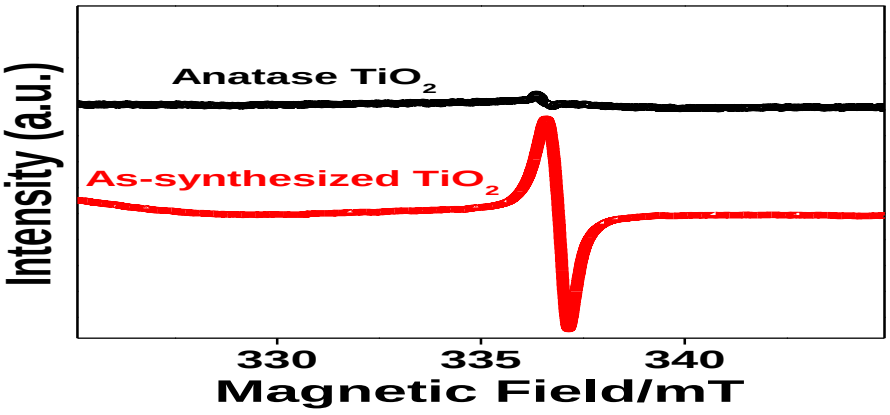

Figure 12 EPR of TiO_2 compared to commercial TiO_2

To verify the presence of Ti^{3+} (or Oxygen vacancies), Electron Paramagnetic Resonance Spectroscopy (EPR) of the as-synthesized TiO_2 and commercial TiO_2 samples conducted as shown in Figure 12. Characteristic EPR signal on the g<2 (g less than 2) region were observed and attributed to Ti^{3+}.

3.1.9 Reduced graphene oxide characterization:

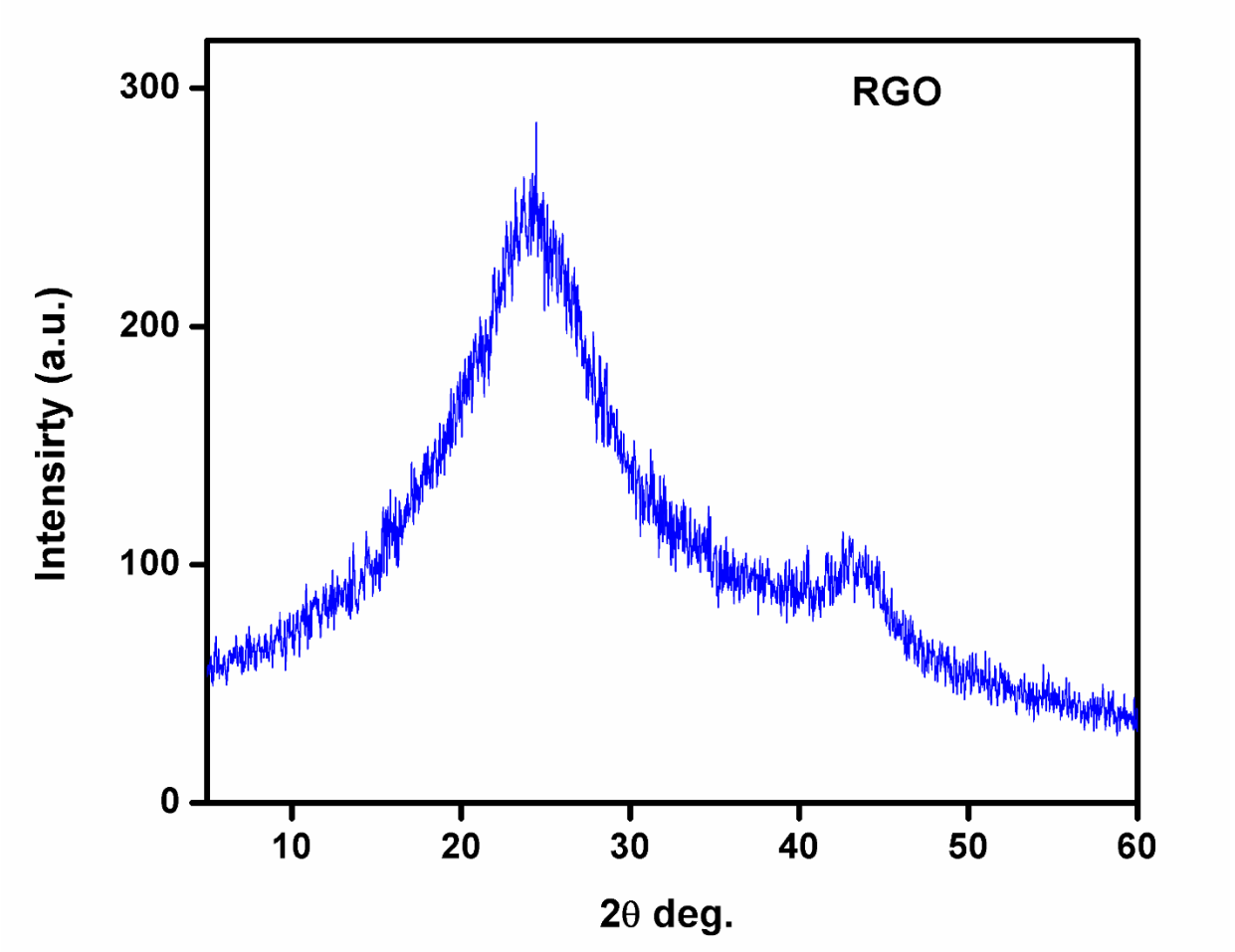

Figure 13 XRD of RGO

The XRD pattern in Figure 13 of the as synthesized reduced graphene oxide (RGO) shows a broad diffraction peak at 23.5° assigned to the (002) reflection of graphene, indicating the reduction process during the hydrothermal treatment, and this indicating the role of benzyl alcohol as a reducing agent. The very broad nature of (002) reflection suggesting poor ordering of nanosheets along the stacking direction[45].

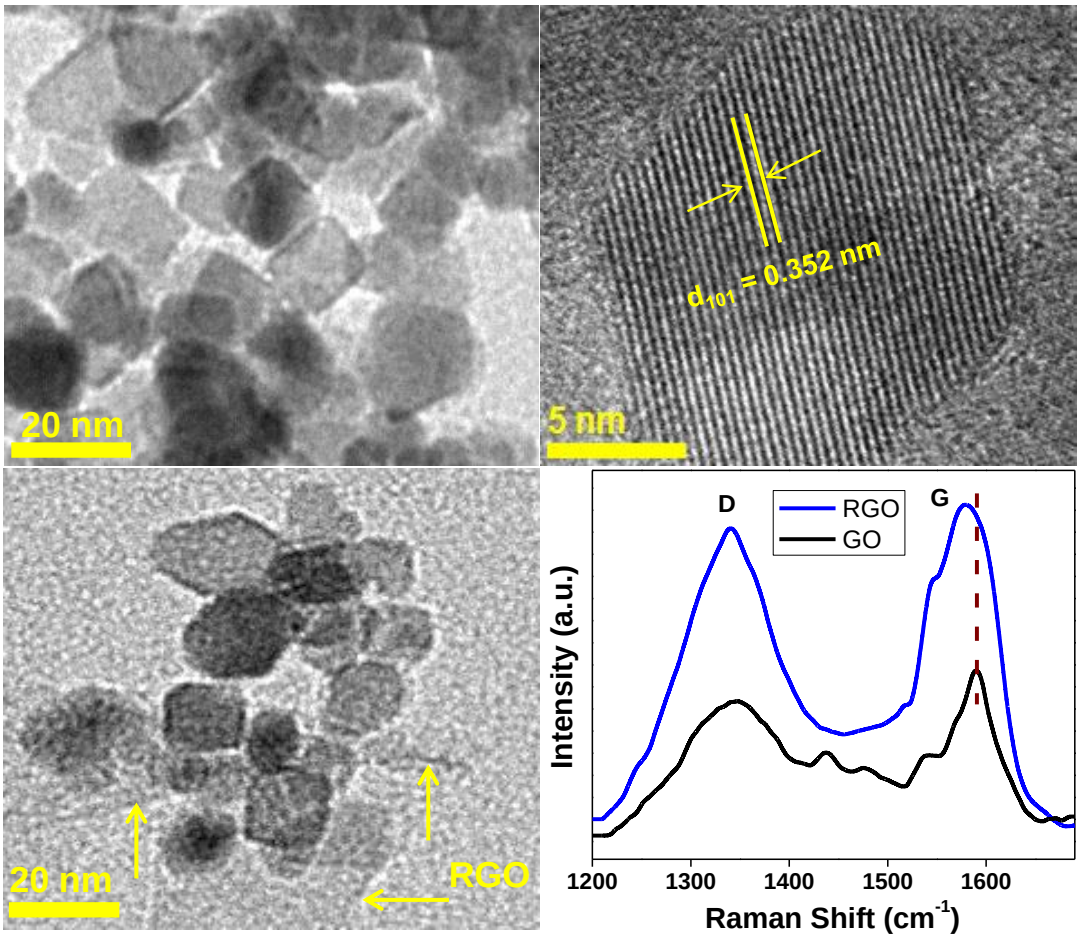

Figure 14 TEM & Raman of the RGO.

The TEM results in Figure 14 provide a direct evidence that the TiO_2 nanoparticles are on the surface of the reduced graphene oxide sheets. The measured d-spacing of 0.352 nm corresponds to (101) of Titania.

Raman spectrum (using Horiba Spectrometer iHR320), illustrate a blue-shift of the G-band, which demonstrate a partial reduction of graphene oxide, and this is a further confirmation in addition to XRD pattern in Figure 13.

3.1.10 Photoelectrocatalytic Activity (PEC):

The photoelectrocatalytic activity studied in a three-electrode cell (Pt as a Counter electrode and calomel as a reference electrode) connected to a potentiostat (273A PAR) as Figure 12 shows, using Sodium sulfate 0.5M as an electrolyte, and the sunlight simulator with wavelength larger than 420 nm with 100% intensity. The catalyst load used 1 mg/cm^2, and voltage sweeping between -0.2 to 1.2 V, with scan rate 10 mV/point.

A 300 W xenon lamp with a cutoff filter to obtain radiation of $\lambda > 420$ nm was used. The light intensity was measured to be 300 mW/cm^2.

The potential sweeps were performed at a rate of 5 mV s^{-1} in all the experiments.

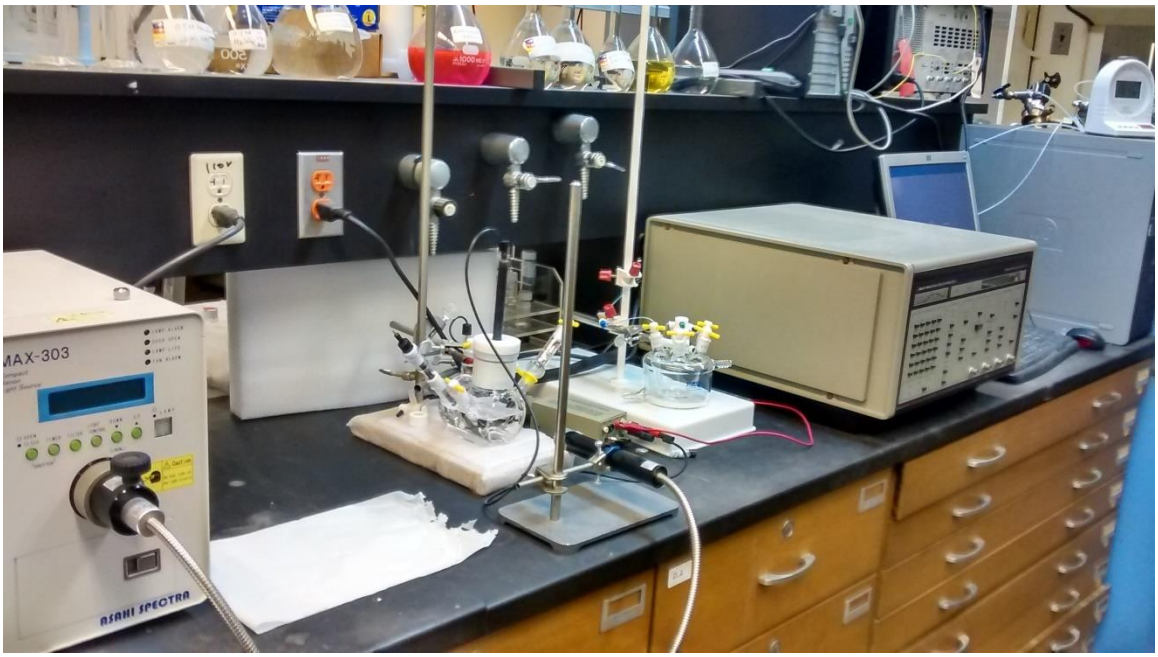

Figure 15 Photoelectrochemical setup.

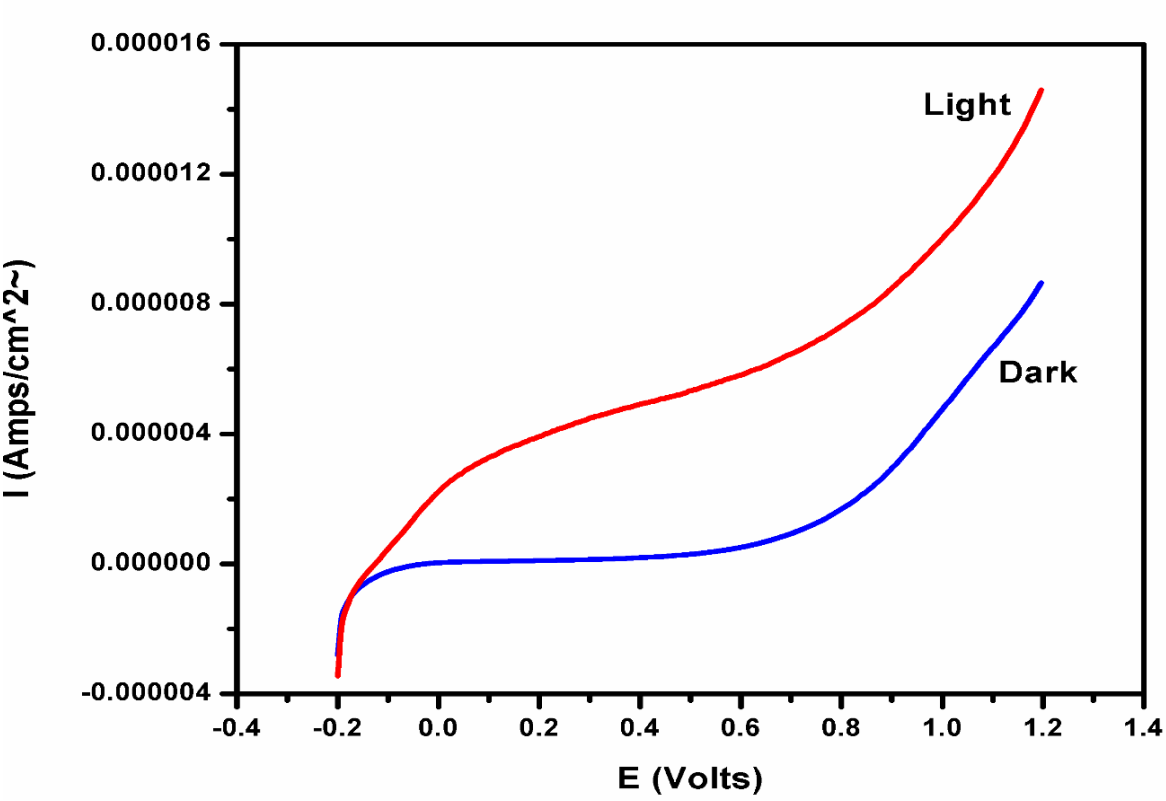

Figure 16 Response of pure TiO_2 under Light and Dark.

Figure 16 shows the photocurrent generated by pure Titania under dark and light, although TiO_2 has dark current, a simple comparison of the photocurrent generated in both states at 0.6 Volt, we can see clearly that the photocurrent generated under light is four times that produced under dark.

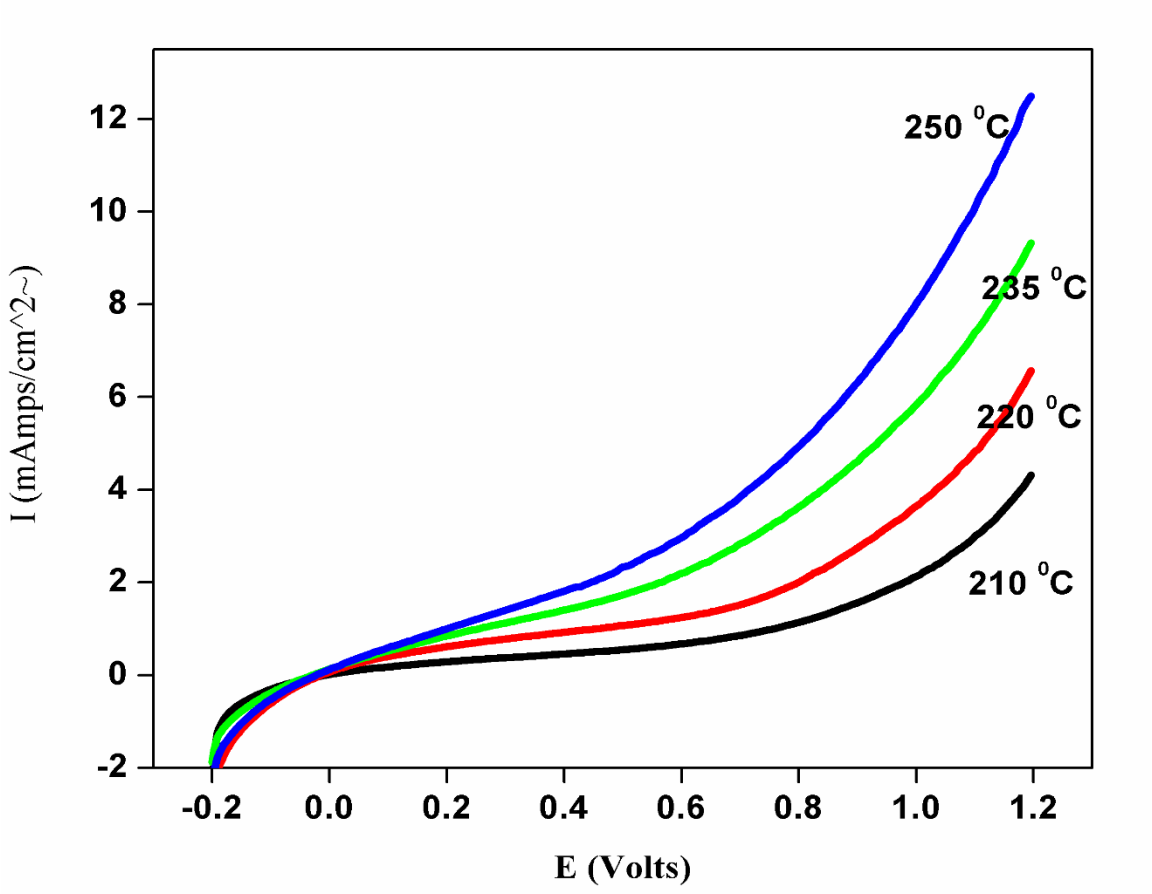

Figure 17 Activity of pure TiO_2 prepared under different temperatures.

Figure 16 showing that the prepared pure Titania in BA has photocatalytic activity under light higher than without light.

While Figure 17 proofed that the photocatalytic activity increase as the synthesis temperature increased, and the TiO_2 prepared under 250 ^{0}C gave the best activity. And the photocurrent produced from 250 ^{0}C sample is three times higher than what produced in 210 ^{0}C sample.

So, the optimum reaction temperature is 250 ^{0}C.

For reaction time, we found that the optimum reaction time is 24 hours as shown in Figure 18.

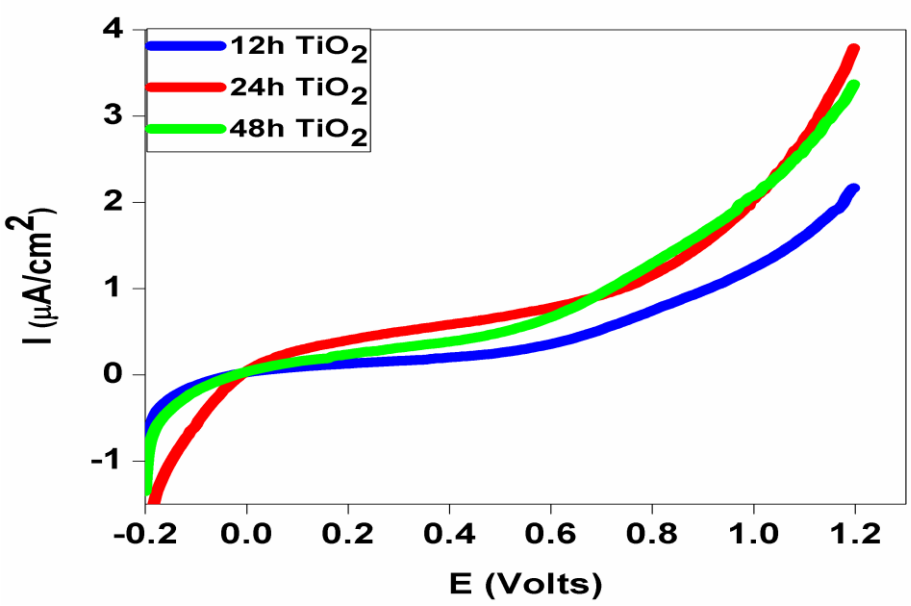

Figure 18 Reaction time effect

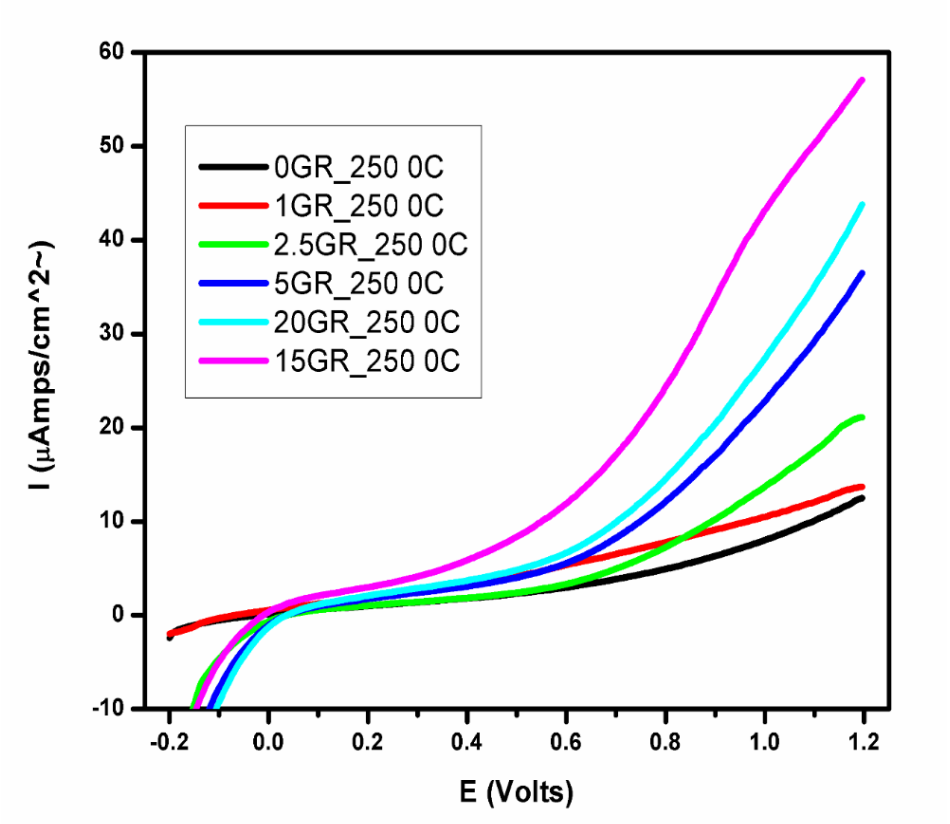

Figure 19 activity of nanocomposites with different RGO load.

Figure 19 illustrates the photocatalytic activity of the TiO_2/RGO nanocomposites with different percentage of reduced graphene oxide, the photocatalytic activity almost increases as we increase graphene oxide percentage until it gives the highest photocurrent with 15% sample and after that drop.

Thus, the optimum reduced graphene oxide weight percentage are 15%.

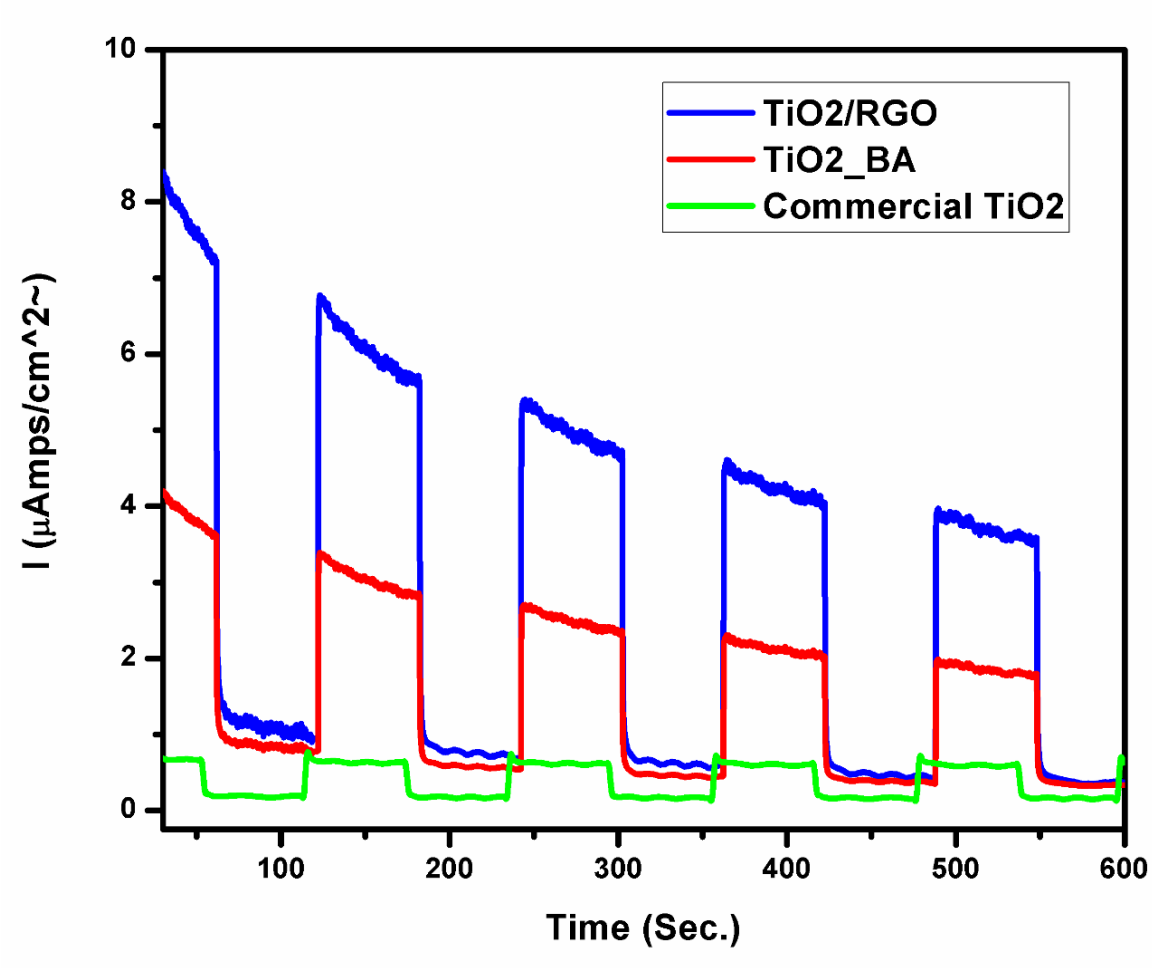

Figure 20 Comparative photocurrent of commercial, pure TiO_2 and TiO_2/RGO

Figure 20 shows that TiO_2/RGO nanocomposite present higher photocurrent than as-synthesized pure TiO_2, and both (TiO_2/RGO & TiO_2_BA) produced much higher photocurrent compared to commercial TiO_2. Moreover, TiO_2/RGO and TiO_2_BA samples showing an obvious decay following the initial fast increase photocurrents, suggesting onset recombination, while we don't see this character in case of commercial TiO_2.

3.2 WO3/RGO Nanocomposites and photocatalytic activity:

3.2.1 WO_3 Synthesis:

0.8 mmol from Tungsten(vi)chloride which typically equal 0.32 g, mixed with 20 ml from Benzyl Alcohol (BA) with vigorous steering until we get a clear solution, Then, the resulting solution transferred to a 45 ml Teflon hydrothermal vessel autoclave and heat it for different temperatures (210 ^{0}C, 220 ^{0}C, 235 ^{0}C and 250 ^{0}C) and times (12h, 24h, 36h, and 48h) for optimization. At the end of the reaction, the obtained product washed five times using acetone (40 ml, three times) and ethanol (25 ml, two times) followed by centrifugation every time for 12000 RPM. Finally, the washed product dried overnight and collected.

3.2.2 WO_3/RGO Synthesis:

Calculated amount from Reduced Graphene Oxide (RGO) dissolved in (BA) by sonication for three hours, taking exact millimeters from this solution depend on the percentage of RGO needed in the nanocomposite (0.5%, 1.0%, 30%, 40% and 50%), then mixed with 0.8 mmol from Tungsten(vi)chloride which typically equal 0.32 g, mixed with (20 ml – the millimeters from BA used with RGO) from Benzyl Alcohol (BA) with vigorous steering until we get a clear yellow solution, Then, the resulting solution transferred to a 45 ml Teflon hydrothermal vessel autoclave and heat it for different temperatures (210 ^{0}C, 220 ^{0}C, 235 ^{0}C and 250 ^{0}C) and times (12h, 24h, 36h and 48h) for optimization. At the end of the reaction, the obtained product washed five times using acetone (40 ml, three times) and ethanol (25 ml, two times) followed by centrifugation every time for 12000 RPM. Finally, the washed product dried overnight and collected.

3.2.3 WO3 XRD:

The formation of monoclinic Tungsten oxide has been proved by XRD with large diffraction intensities of the (002), (020) and (200) facets as Figure 21 showing well-defined diffraction pattern of the as-synthesized Tungsten oxide at 250 ^{0}C for long time (48hours), and it's typically fit with entry No (ICDD 96-210-6383).

The crystal has a monoclinic unit cell with a=7.3060 Å, b=7.5400 Å, c=7.6920 Å, β=90.881 °. The diffraction peaks at 2Θ=23.11 ^{0}, 23.57 ^{0}, and 24.35 ^{0} correspond to (002), (020) and (200) facets respectively. All diffraction peaks are indexed to the monoclinic phase of WO_3 indicating that the product has high purity.

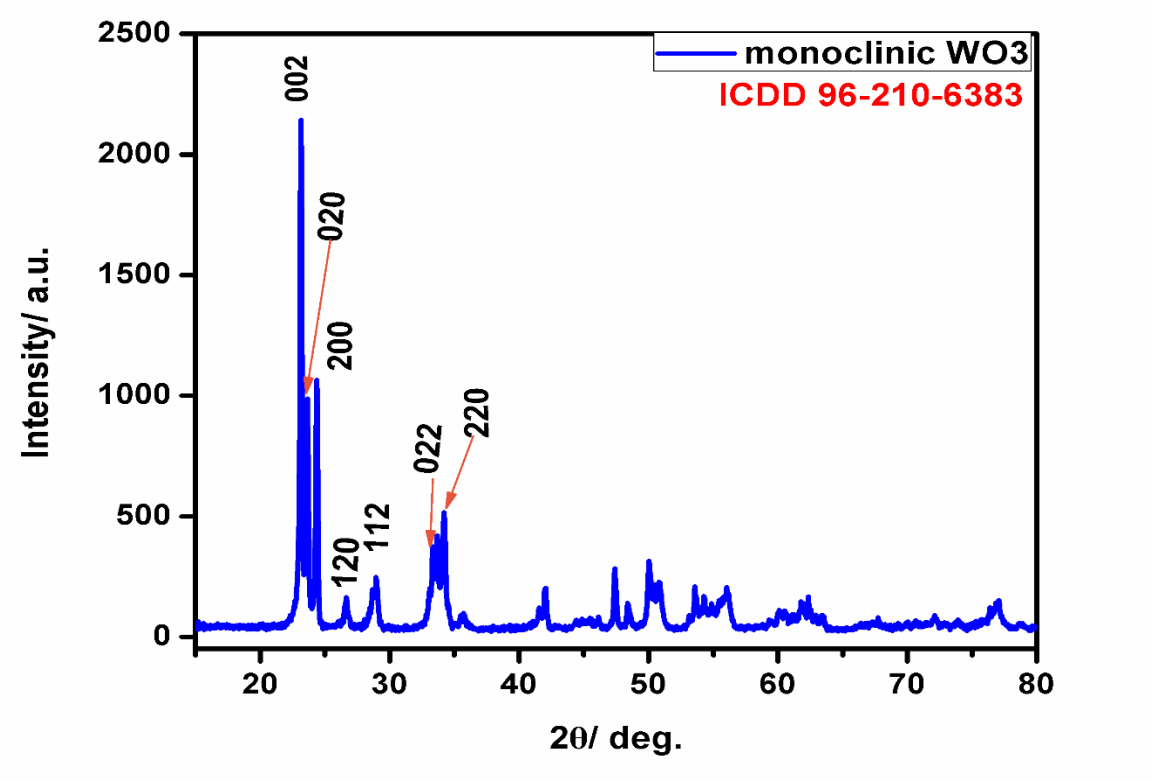

Figure 21 XRD pattern of pure WO_3

3.2.4 WO_3 and WO_3/RGO TEM:

More detailed crystal structural information on the as-prepared Tungsten Oxide and Tungsten oxide nanocomposite with reduced graphene oxide were carried out by TEM.

WO_3 nanoparticles ranging from 40 to 60 nm appeared in the TEM images, with little distorted cubic morphologies. d-spacing of 0.384 nm corresponds to (002) facets.

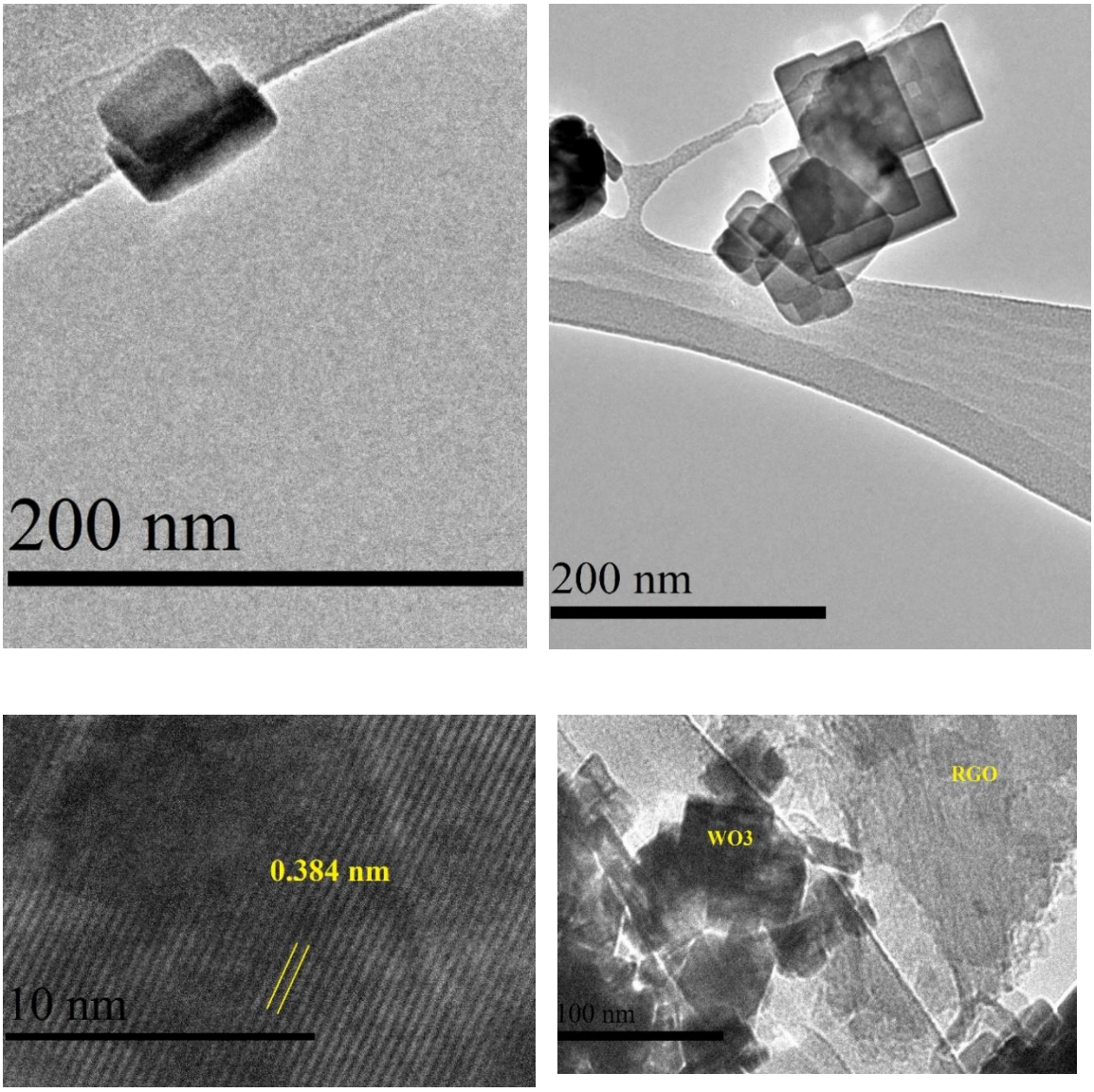

Figure 22 TEM of WO_3 & WO_3/RGO

3.2.5 Photocatalytic activity

To study the photocatalytic activity of the as-synthesized Tungsten Oxide and Tungsten oxide nanocomposites with reduced graphene oxide, and to know the optimum condition, several parameters have been considered, such as the precursor amount, reaction time, reaction temperature and reduced graphene oxide content.

But first let us compare the photocurrent produced un dark and under light to see to how extend light is important for getting high photocurrent.

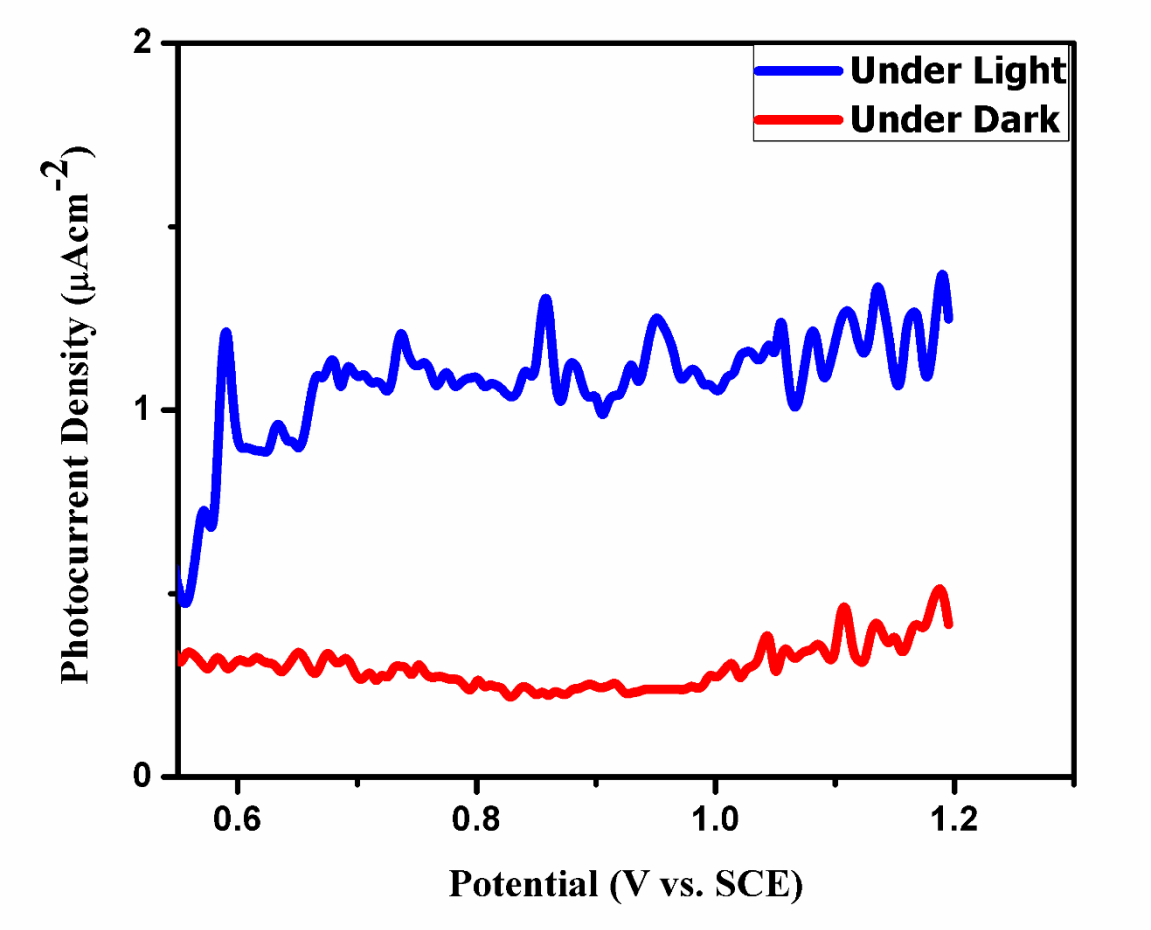

Figure 23 WO3_BA under light & dark

As Figure 23 shows the photocurrent obtained from pure as prepared Tungsten Oxide under light is twice the current obtained under dark.

On the other hand, the photocurrent produced from Tungsten Oxide/Reduced Graphene Oxide nanocomposite under light and dark are almost the same as Figure 24 illustrate, that mean light has almost no effect on the photocurrent produced for the nanocomposite and it's light inactive.

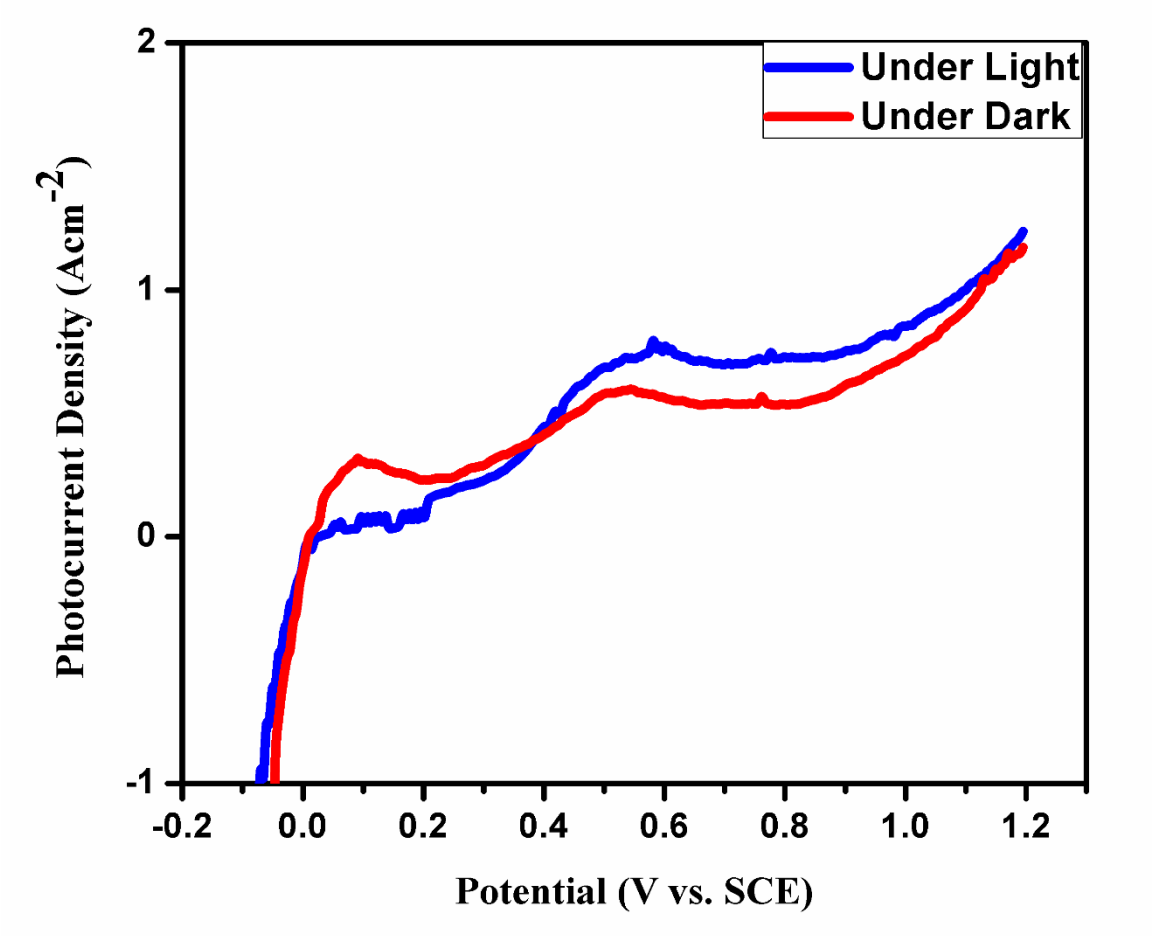

Figure 24 WO3/RGO under Light & Dark

3.2.5.1 Precursor amount:

We tried several amounts from Tungsten hexachloride to select the optimum precursor amount, and it's worth mentioning here that we only checked four different amounts because as we increase the precursor content we end up with various unknown polymeric sticky material very difficult to remove from the hydrothermal vessel.

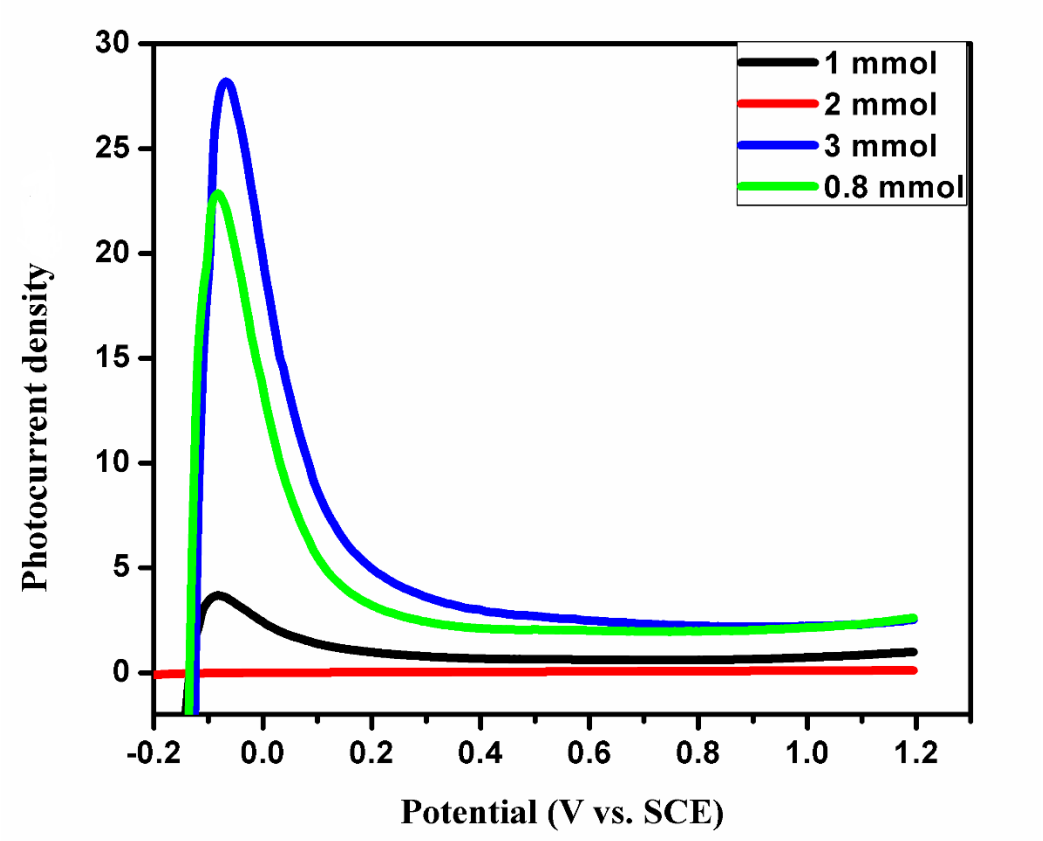

Figure 25 Effect of precursor content on the photocatalytic activity.

To check the effect of the precursor content we fixed the temperature on 220 ^{0}C and the reaction time 24 hours. although the experiment started with 3.0 *mmol* gave the highest photocurrent as Figure 25 shows, but the unknown sticky material appeared with a huge amount. Fortunately, the reaction started with 0.8 *mmol* from the precursor give almost the

same photocurrent, so we found that the optimum reaction precursor amount is 0.8 *mmol* which is typically equal 0.317 gram.

3.2.5.2 Catalyst load:

On the methodology about working electrode preparation, we said we used to deposit 1 mg from the catalyst on 1 cm^2 of Indium Tin Oxide coated glass.

But the catalyst load might affect the photocatalytic activity, for that reason we optimized this parameter, and Figure 26 show, the optimum catalyst load is 1.0 mg/cm^2 although the different is not high compared to other amounts used. And the decrease on the photocurrent observed as we increase the catalyst load could be attributed to the difficulty that face the electrons and holes to reach the catalyst surface due to the thickness of the catalyst layer and this result on accelerating the recombination process of the electrons and holes as well as blocking the active sites.

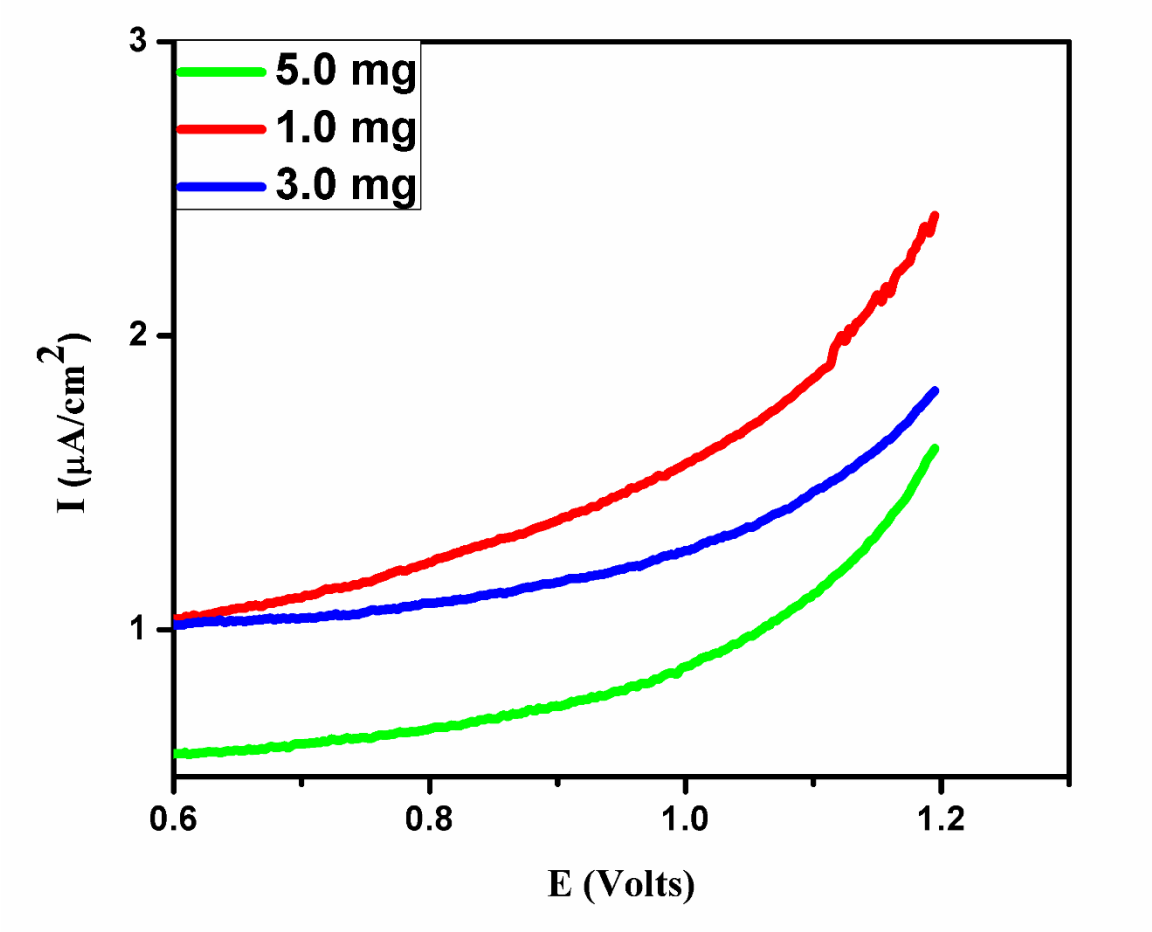

Figure 26 Catalyst load effect

3.2.5.3 Reaction Temperature:

One important parameter of the optimization process are the temperature, but in our reaction, we do not have wide range from temperatures since the boiling point of the solvent benzyl alcohol are 205 ^{0}C and our hydrothermal vessels can afford temperatures up to 250 ^{0}C, so selected four different temperatures 210 ^{0}C, 220 ^{0}C, 235 ^{0}C and 250 ^{0}C.

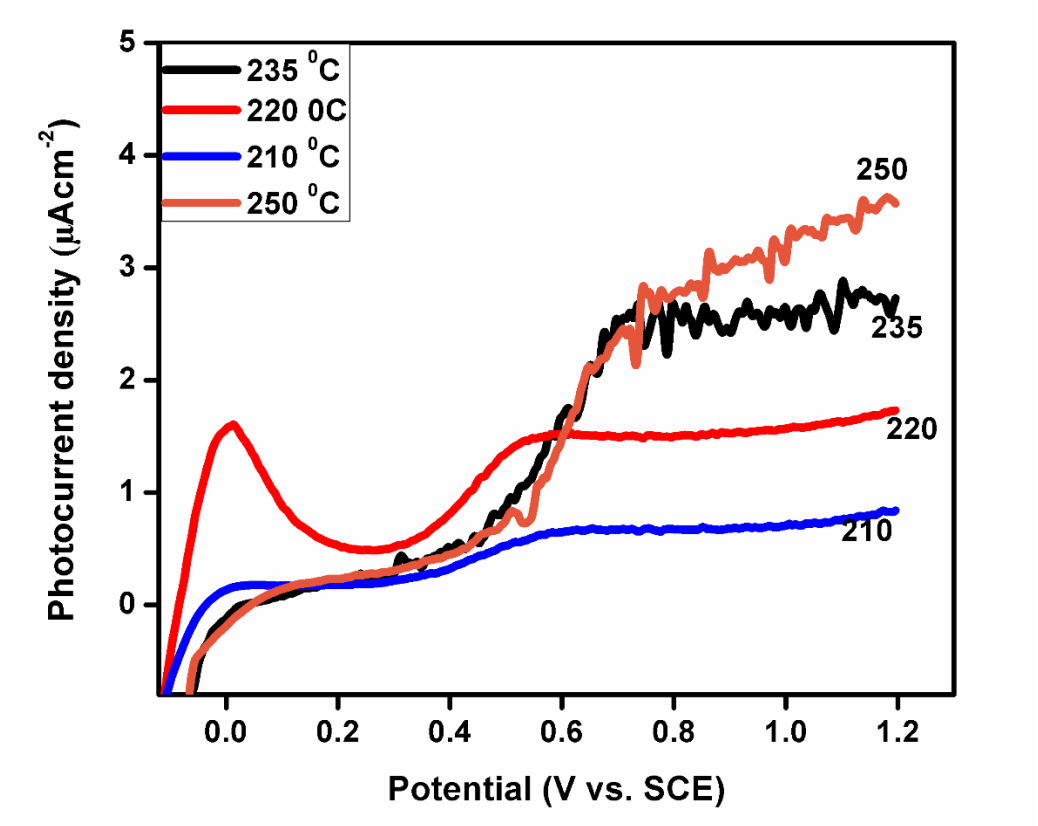

Figure 27 The Effect of temperature

As Figure 27 illustrate the optimum reaction temperature are 250 ^{0}C. The photocurrent generated by the reaction under 250 ^{0}C is almost three times higher than that produced under 210 ^{0}C.

3.2.5.4 Reaction Time:

To optimize the reaction time, we fixed the precursor amount on 0.8 *mmol*, and the temperature at 250 ^{0}C, and then we run the reaction for 12h, 24h, 36h and 48h. as we can see in Figure 28 no huge difference on the current produced have been noticed as we changing the reaction time, yet running the reaction for 48 hours gave the best current density.

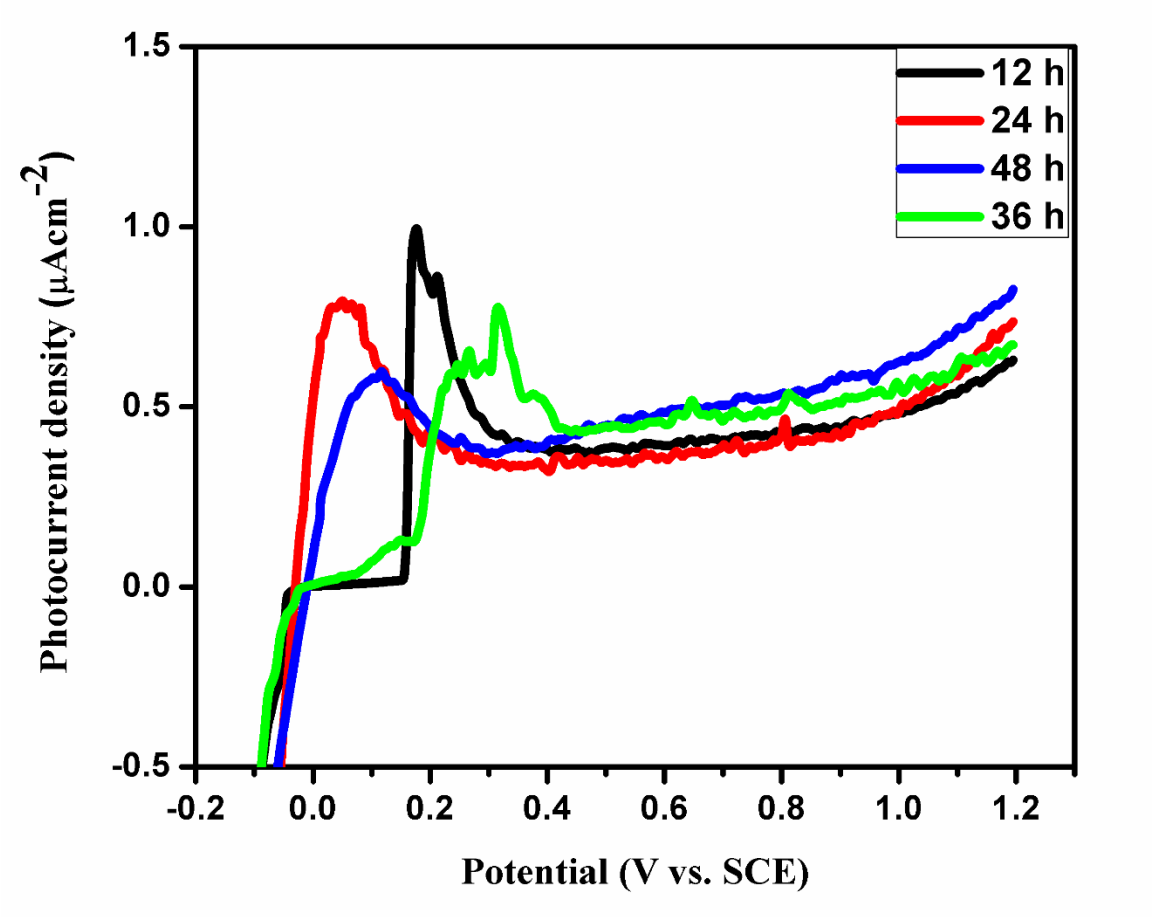

Figure 28 the effect of reaction time

3.2.5.5 Reduced Graphene Oxide content:

In case of reduced graphene oxide composites with Titania, Zhang *et al* came to conclusion that as the graphene content exceed 5 wt% in GR/TiO_2 composite, the photocatalytic activity would decrease clearly, but in case of GR/WO3 composites Guo *et al* reported the highest photocatalytic activity for their nanocomposite (GR/WO_3) with graphene content 40 wt%.[42]

So, we prepared five different WO_3/RGO nanocomposites with different RGO content, three of them with high percentages 30 wt%, 40 wt% and 50 wt% and two with small RGO content 0.5 wt% and 1.0 wt%.

As Figure 29 illustrates very small photocurrent generated from the nanocomposites in both cases, whether RGO with high or low content.

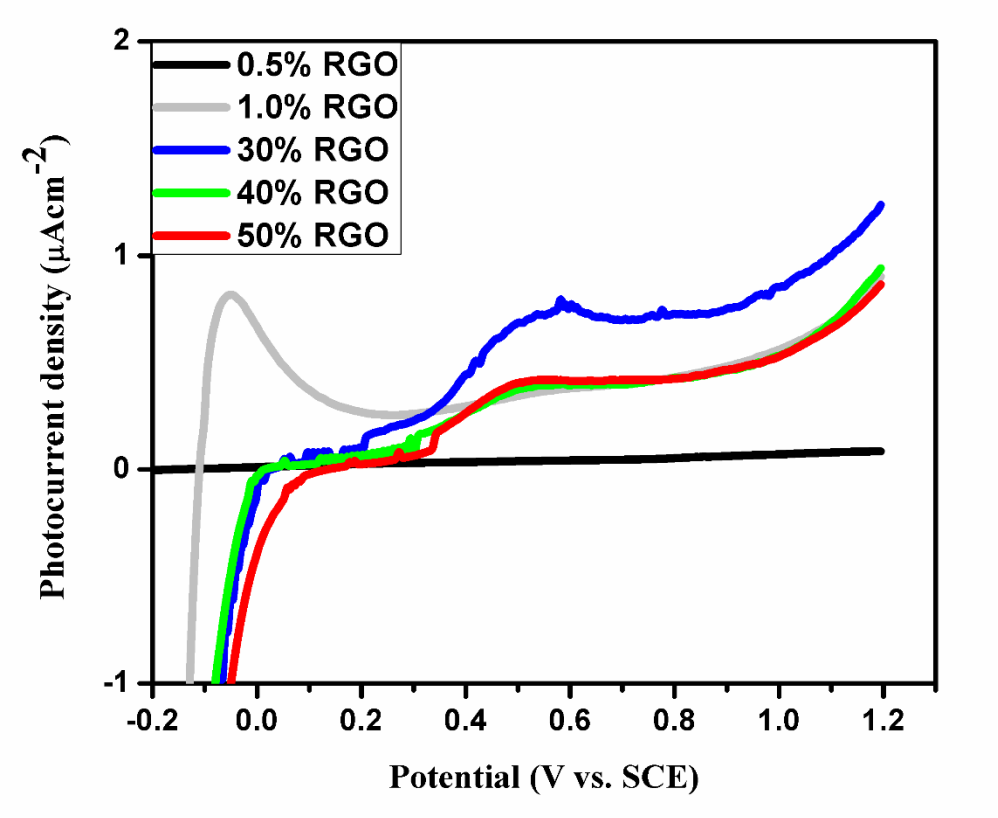

Figure 29 The effect of RGO content

3.2.5.6 On/Off experiment:

Figure 30 shows the variation of photocurrent under illumination and dark condition by switching the light on and off for 10 min (20 second ON and 20 second OFF) at a constant applied voltage 1.1 Volt, here we studied the best 2 samples with and without RGO, it clearly appears that the photocurrent generated by pure WO_3 is more than 3 times higher than that produced by WO_3/RGO 30%.

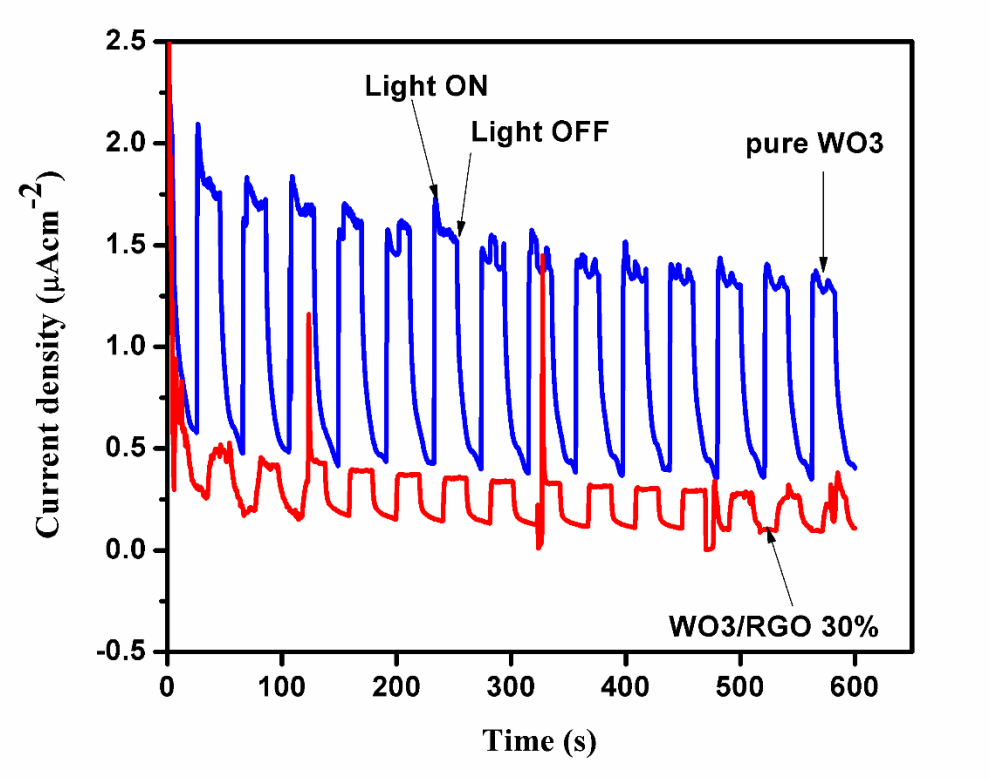

Figure 30 Comparative photocurrent profile at 1.1 Volt.

CHAPTER 4

Conclusion and Recommendation

4.1 Conclusion:

"Benzyl alcohol route" is an effective and simple one-step approach, used to synthesize highly crystalline anatase TiO_2 and monoclinic WO_3.

TiO_2 and WO_3 and their nanocomposites with RGO have been also synthesized in one step, characterized and their photocatalytic activity was studied. Benzyl alcohol played several roles, as solvent, shaping agent and a reducing agent.

And since the boiling point of benzyl alcohol is 205 ^{0}C, and the Teflon hydrothermal vessel autoclave we used can bear temperatures until 250 ^{0}C safely, so we synthesized our pure TiO_2 and WO_3 and their nanocomposites with RGO in different four temperatures which are 210 ^{0}C, 220 ^{0}C, 235 ^{0}C and 250 ^{0}C. Also, we optimized the reaction time and did the reaction for 12h, 24h, 36h, and 48h. graphene oxide content and the catalyst load have been optimized also. In the case of TiO_2, we found that the optimum condition is reaction time are 24h, reaction temperature 250 ^{0}C, and 15% RGO. TiO_2 with 15% RGO gave the highest current (~58 μAcm^{-2}), which is six times higher than the prepared pure TiO_2.

While in WO_3 case we found that the optimum condition is 48 h reaction time, 250 ^{0}C reaction temperature and 30% RGO weight percentage. WO_3 prepared at 250 ^{0}C for 48h gave the highest current (4 μAcm^{-2}), which approximately four times higher than the photocurrent generated by the sample with RGO (30% RGO).

4.2 Recommendations:

Other metal oxides can be synthesized using the same approach “benzyl alcohol route”. As well as a combination of two metal oxides or more can be synthesized using the same method.

Use the metal oxide synthesized by this approach for different applications such as gas sensing and desulfurization.

The detailed kinetic study is recommended for a deep understanding of reaction mechanism.

Nanocomposites of metal oxides and other carbonaceous material than RGO is recommended to be synthesized by the same method whether for photoelectrochemical water splitting or other applications.

References

[1] N. Abas, A. Kalair, and N. Khan, "Review of fossil fuels and future energy technologies," *Futures*, vol. 69, pp. 31–49, 2015.

[2] L. M. Peter, "Photoelectrochemical Water Splitting. A Status Assessment," *Electroanalysis*, p. n/a-n/a, 2015.

[3] X. Zou and Y. Zhang, "Noble metal-free hydrogen evolution catalysts for water splitting," *Chem. Soc. Rev.*, 2015.

[4] P. Szymanski and M. a. El-Sayed, "Some recent developments in photoelectrochemical water splitting using nanostructured TiO 2: A short review," *Theor. Chem. Acc.*, vol. 131, no. 6, pp. 1–12, 2012.

[5] V. H. Nguyen and B. H. Nguyen, "Visible light responsive titania-based nanostructures for photocatalytic, photovoltaic and photoelectrochemical applications," *Adv. Nat. Sci. Nanosci. Nanotechnol.*, vol. 3, no. 2, p. 23001, 2012.

[6] N. S. Lewis, G. Crabtree, A. J. Nozik, M. R. Wasielewski, and P. Alivisatos, "Basic Research Needs for Solar Energy Utilization," *Basic Energy Sci. Work. Sol. Energy Util.*, p. 276, 2005.

[7] C. Letters, H. Reviews, H. Review, and P. Commentary, "Preparing Articles on Photocatalysis — Beyond the Illusions , Misconceptions , and Speculation," vol. 37, no. 3, pp. 216–229, 2008.

[8] A. G. Muñoz, "Monolithic Solar Water-Splitting Systems : Towards a Sustainable Hydrogen-Energy Future," pp. 1–14, 2014.

[9] M. Grätzel, "Photoelectrochemical cells.," *Nature*, vol. 414, no. 6861, pp. 338–344, 2001.

[10] S. Licht, O. Khaselev, P. a Ramakrishnan, T. Soga, and M. Umeno, "Multiple-Bandgap Photoelectrochemistry: Bipolar Semiconductor Ohmic Regenerative Electrochemistry," *J. Phys. Chem. B*, vol. 102, no. 98, pp. 2536–2545, 1998.

[11] a. H. Almasoud and H. M. Gandayh, "Future of solar energy in Saudi Arabia," *J. King Saud Univ. - Eng. Sci.*, vol. 27, no. 2, pp. 153–157, 2014.

[12] S. H. Alawaji, "Evaluation of solar energy research and its applications in Saudi Arabia — 20 years of experience," *Renew. Sustain. Energy Rev.*, vol. 5, no. 1, pp. 59–77, 2001.

[13] A. Kudo and Y. Miseki, "Heterogeneous photocatalyst materials for water splitting.," *Chem. Soc. Rev.*, vol. 38, no. 1, pp. 253–278, 2009.

[14] N. Pinna, "The ?benzyl alcohol route?: an elegant approach towards organic?inorganic hybrid nanomaterials," *J. Mater. Chem.*, vol. 17, no. 27, p. 2769,

2007.

[15] P. Dong, Y. Wang, L. Guo, B. Liu, S. Xin, J. Zhang, Y. Shi, W. Zeng, and S. Yin, "A facile one-step solvothermal synthesis of graphene/rod-shaped TiO_2 nanocomposite and its improved photocatalytic activity.," *Nanoscale*, vol. 4, no. 15, pp. 4641–4649, Aug. 2012.

[16] J. William S. Hummers and R. E. Offeman, "Preparation of Graphitic Oxide," *J. Am. Chem. Soc*, vol. 80, no. 1937, p. 1339, 1958.

[17] T. Bak, J. Nowotny, M. Rekas, and C. . Sorrell, "Photo-electrochemical hydrogen generation from water using solar energy. Materials-related aspects," *Int. J. Hydrogen Energy*, vol. 27, no. 10, pp. 991–1022, 2002.

[18] M. Niederberger, G. Garnweitner, N. Pinna, and G. Neri, "Non-aqueous routes to crystalline metal oxide nanoparticles: Formation mechanisms and applications," *Prog. Solid State Chem.*, vol. 33, no. 2–4 SPEC. ISS., pp. 59–70, 2005.

[19] D. P. Debecker and P. H. Mutin, "Non-hydrolytic sol-gel routes to heterogeneous catalysts," *Chem. Soc. Rev.*, vol. 41, no. 9, pp. 3624–3650, 2012.

[20] M. Niederberger and G. Garnweitner, "Organic reaction pathways in the nonaqueous synthesis of metal oxide nanoparticles," *Chem. - A Eur. J.*, vol. 12, no. 28, pp. 7282–7302, 2006.

[21] a Fujishima and K. Honda, "Electrochemical photolysis of water at a semiconductor electrode.," *Nature*, vol. 238, no. 5358, pp. 37–38, 1972.

[22] Y. Cong, M. Long, Z. Cui, X. Li, Z. Dong, G. Yuan, and J. Zhang, "Anchoring a uniform TiO2 layer on graphene oxide sheets as an efficient visible light photocatalyst," *Appl. Surf. Sci.*, vol. 282, pp. 400–407, Oct. 2013.

[23] G. Wang, Y. Ling, and Y. Li, "Oxygen-deficient metal oxide nanostructures for photoelectrochemical water oxidation and other applications.," *Nanoscale*, vol. 4, no. 21, pp. 6682–91, Nov. 2012.

[24] G. L. Chiarello and E. Selli, *Photocatalytic production of hydrogen*. Woodhead Publishing Limited, 2014.

[25] D. Dambournet, I. Belharouak, and K. Amine, "Tailored preparation methods of TiO2 anatase, rutile, brookite: Mechanism of formation and electrochemical properties," *Chem. Mater.*, vol. 22, no. 3, pp. 1173–1179, 2010.

[26] J. A. Byrne, P. a. Fernandez-Ibañez, P. S. M. Dunlop, D. M. a Alrousan, and J. W. J. Hamilton, "Photocatalytic enhancement for solar disinfection of water: A review," *Int. J. Photoenergy*, vol. 2011, 2011.

[27] B. Wawrzyniak, A. W. Morawski, and B. Tryba, "Preparation of TiO2-nitrogen-doped photocatalyst active under visible light," *Int. J. Photoenergy*, vol. 2006, pp. 1–8, 2006.

[28] R. Leary and A. Westwood, "Carbonaceous nanomaterials for the enhancement of TiO2 photocatalysis," *Carbon N. Y.*, vol. 49, no. 3, pp. 741–772, 2011.

[29] K. S. Novoselov, a K. Geim, S. V Morozov, D. Jiang, Y. Zhang, S. V Dubonos, I. V Grigorieva, and a a Firsov, "Electric field effect in atomically thin carbon films.," *Science*, vol. 306, no. 5696, pp. 666–669, 2004.

[30] A. H. Castro Neto, "The carbon new age," *Mater. Today*, vol. 13, no. 3, pp. 12–17, 2010.

[31] A. Adán-Más and D. Wei, "Photoelectrochemical Properties of Graphene and Its Derivatives," *Nanomaterials*, vol. 3, no. 3, pp. 325–356, 2013.

[32] G. Williams, B. Seger, and P. V Kamat, "UV-Assisted Photocatalytic Reduction of Graphene Oxide," vol. 2, no. 7, pp. 1487–1491, 2008.

[33] K. K. Manga, S. Wang, M. Jaiswal, Q. Bao, and K. P. Loh, "High-gain graphene-titanium oxide photoconductor made from inkjet printable ionic solution," *Adv. Mater.*, vol. 22, no. 46, pp. 5265–5270, 2010.

[34] S. Bai and X. Shen, "Graphene–inorganic nanocomposites," *RSC Adv.*, vol. 2, no. 1, p. 64, 2012.

[35] M. C. Rao, "Structure and Properties of Wo 3 Thin Films for Electrochromic Device Application," *J. Non-Oxide Glas.*, vol. 5, no. 1, pp. 1–8, 2013.

[36] "© 1976 Nature Publishing Group," 1976.

[37] S. Sfaelou, L. C. Pop, O. Monfort, V. Dracopoulos, and P. Lianos, "Mesoporous WO3 photoanodes for hydrogen production by water splitting and PhotoFuelCell operation," *Int. J. Hydrogen Energy*, vol. 41, no. 14, pp. 5902–5907, 2016.

[38] J. Zhang, P. Zhang, T. Wang, and J. Gong, "Monoclinic WO3 nanomultilayers with preferentially exposed (002) facets for photoelectrochemical water splitting," *Nano Energy*, vol. 11, pp. 189–195, 2015.

[39] J. Gan, X. Lu, and Y. Tong, "Towards highly efficient photoanodes: boosting sunlight-driven semiconductor nanomaterials for water oxidation.," *Nanoscale*, vol. 6, pp. 7142–64, 2014.

[40] X. Liu, F. Wang, and Q. Wang, "Nanostructure-based WO3 photoanodes for photoelectrochemical water splitting," *Phys. Chem. Chem. Phys.*, vol. 14, pp. 7894–7911, 2012.

[41] J. Lin, P. Hu, Y. Zhang, M. Fan, Z. He, C. K. Ngaw, J. S. C. Loo, D. Liao, and T. T. Y. Tan, "Understanding the photoelectrochemical properties of a reduced graphene oxide–WO3 heterojunction photoanode for efficient solar-light-driven overall water splitting," *RSC Adv.*, vol. 3, no. 24, p. 9330, 2013.

[42] J. Guo, Y. Li, S. Zhu, Z. Chen, Q. Liu, D. Zhang, W.-J. Moon, and D.-M. Song,

"Synthesis of WO 3 @Graphene composite for enhanced photocatalytic oxygen evolution from water," *RSC Adv.*, vol. 2, no. 4, pp. 1356–1363, 2012.

[43] B. Y. S. Chang, M. S. Mehmood, A. Pandikumar, N. M. Huang, H. N. Lim, A. R. Marlinda, N. Yusoff, and W. S. Chiu, "Hydrothermally prepared graphene-titania nanocomposite for the solar photocatalytic degradation of methylene blue.," *Desalin. Water Treat.*, vol. 3994, no. March, p. Ahead of Print, 2015.

[44] Y.-F. Li, U. Aschauer, J. Chen, and A. Selloni, "Adsorption and Reactions of O2 on Anatase TiO2.," *Acc. Chem. Res.*, Apr. 2014.

[45] C. Nethravathi and M. Rajamathi, "Chemically modified graphene sheets produced by the solvothermal reduction of colloidal dispersions of graphite oxide," *Carbon N. Y.*, vol. 46, no. 14, pp. 1994–1998, 2008.

Vitae

Name: MOHAMMED ABDALWADOUD

Nationality: SUDANESE

Date of Birth: 7/3/1987

Email: abdalwdoud87@gmail.com

g201206780@kfupm.edu.sa

Address: Dhahran - Saudi Arabia

Academic Background: B.Sc. (Honor) in Chemistry - Sudan University of Science and Technology 2008

Work Experiences: Almajd Private Secondary Schools(boys/girls)

Chemistry Teacher (Feb 2010 – Jan 2013)

: Hassnain Private School Foundation

Chemistry Teacher (Oct 2010 – Jan 2013)

Publications: Single-Pot Synthesis of ⟨001⟩-Faceted N-doped Nb_2O_5/Reduced Graphene Oxide Nanocomposites for Efficient Photoelectrochemical Water Splitting.

M. Qamar, **M. Abdalwadoud**, M. I. Ahmed, A.- M. Azad,

B. Merzougui, S. Bukola, Z. H. Yamani, and M. N. Siddiqui

Conferences: Attended The 4th Saudi International Nanotechnology Conference (SINC 2016), Oct 25 – 27, 2016.
Attended The 3rd Saudi International Nanotechnology Conference (3SINC) Dec 1 – 3, 2014.

Courses: Neuro Linguistic Programming Diploma
Feb 20 – 23, 2012.

Part time jobs: Lab Technical Support Office (LTSO).
Term 151.
Chemistry Department.
Administrative Assistance, Term 141.

Training: SciFinder, your first step in the scientific research.
Saudi Digital Library, May 2, 2017.
How to publish a scientific paper with Wiley.
Saudi Digital Library, May 16, 2017.

ICP-MS, Chemistry Department, KFUPM.
May 24-25, 2015.

Atomic Force Microscopy, Chemistry Department, KFUPM.

April 4, 2016.

Introduction in Latex, Graduate Students Club, KFUPM.

March 9, 2016.

Quantum Chemistry, Chemistry Department, SUST.

Jan-July 2012.